Energy Research and Development Division
FINAL PROJECT REPORT

Demonstration and Validation of PV Output Variability Modeling Approach

Prepared for: California Energy Commission
Prepared by: Clean Power Research

JULY 2013
CEC-500-10-059

Prepared by:

Primary Author(s):
Thomas E. Hoff
Benjamin L. Norris
Phil Gruenhagen
David Chalmers
Andrew Parkins

Clean Power Research
1700 Soscol Avenue, Suite 22
Napa, CA 94559
425.242.4174
www.cleanpower.com

Contract Number: **CEC 500-10-059**

Prepared for:

California Energy Commission

Zhiqin Zhang
Contract Manager

Linda Spiegel
Office Manager
Energy Efficiency Research Office

Laurie ten Hope
Deputy Director
ENERGY RESEARCH AND DEVELOPMENT DIVISION

Robert P. Oglesby
Executive Director

ACKNOWLEDGEMENTS

This study was funded under the California Energy Commission (CEC)'s Public Interest Energy Research (PIER) program. The project is entitled "Demonstration and Validation of PV Output Modeling Approach". Special thanks to Jim Blatchford from California Independent System Operator (CAISO) for providing data and guidance for the analysis and to direction provided by Smita Gupta from California Solar Initiative (CSI) project manager. Opinions expressed herein are those of the authors only.

PREFACE

The California Energy Commission Energy Research and Development Division supports public interest energy research and development that will help improve the quality of life in California by bringing environmentally safe, affordable, and reliable energy services and products to the marketplace.

The Energy Research and Development Division conducts public interest research, development, and demonstration (RD&D) projects to benefit California.

The Energy Research and Development Division strives to conduct the most promising public interest energy research by partnering with RD&D entities, including individuals, businesses, utilities, and public or private research institutions.

Energy Research and Development Division funding efforts are focused on the following RD&D program areas:

- Buildings End-Use Energy Efficiency
- Energy Innovations Small Grants
- Energy-Related Environmental Research
- Energy Systems Integration
- Environmentally Preferred Advanced Generation
- Industrial/Agricultural/Water End-Use Energy Efficiency
- Renewable Energy Technologies
- Transportation

This is the final report for the Demonstration and Validation of PV Output Variability Modeling Approach project (contract number CEC-500-10-059) conducted by Clean Power Research®. The information from this project contributes to Energy Research and Development Division's Renewable Energy Technologies Program.

For more information about the Energy Research and Development Division, please visit the Energy Commission's website at www.energy.ca.gov/research/ or contact the Energy Commission at 916-327-1551.

ABSTRACT

The California Energy Commission's (CEC) Public Interest Energy Research (PIER) program awarded Clean Power Research a contract to evaluate satellite-derived irradiance and simulated PV fleet performance accuracy for PV resource management in the CAISO control area. The goals of the Agreement are to validate existing research and tools, and to integrate the results into the CAISO's planning process.

Under this research, Clean Power Research® (CPR) has collected a database that includes all of the solar PV systems installed in California and developed a unique method to predict PV fleet power production. SolarAnywhere® FleetView™ uses inputs of satellite-derived solar resource data and the design attributes and locations of PV systems to predict PV fleet power production.

The database includes locations of all PV systems in California. PV fleet power production was simulated using FleetView. Measured PV power production was provided by the CAISO. The measured data was used to identify performance issues and to compare with simulated results.

The PV fleet power production variability modeling results suggest that 3 percent Relative Mean Absolute Error (rMAE) can be achieved for PV fleet simulation for 15-minute time interval data over a six-week period given that accurate location-specific solar resource data is supplied; correct PV specifications are used; the PV simulation model is properly tuned; and PV plant operating status is reflected in the simulation to account for poor performance. Results also suggest that total error was over 7 percent if the model was not tuned and PV plant operating status was not reflected in the simulation.

Keywords: California Energy Commission, California Independent System Operator, Clean Power Research, SolarAnywhere, FleetView, PV production, PV production, PV variability, renewable energy

Please use the following citation for this report:

Hoff, Thomas, Benjamin L. Norris, Phil Gruenhagen. (Clean Power Research). 2013. ***Demonstration and Validation of Output Variability Modeling Approac.*** California Energy Commission. Publication number: CEC-500-2010-059.

TABLE OF CONTENTS

LIST OF FIGURE

LIST OF TABLES

EXECUTIVE SUMMARY

Photovoltaic (PV) plant production variability is a critical challenge to increased PV penetration into California's electricity system. A number of studies have examined the issue of PV output variability (see [1] through [12]). A consistent finding of these studies is that variability is reduced when PV systems are geographically dispersed. That is, variability is reduced as the number of systems increases across a sufficiently large geographic region.

The California Energy Commission's (CEC) Public Interest Energy Research (PIER) program awarded Clean Power Research® (CPR) a contract to evaluate satellite-derived irradiance and simulated PV fleet performance accuracy for PV resource management in the CAISO control area. The goals of this research are to validate existing research and tools, and to integrate the results into the CAISO's planning process. The accuracy of the method needs to be demonstrated for PV sources within the CAISO control area, and data needs to be delivered in a manner compatible with the existing energy and reserve market mechanisms.

Under this research, CPR has collected and delivered to CEC a database that includes all of the solar PV systems installed in California and developed a unique method to predict PV fleet power production variability. The method uses inputs of satellite-derived solar resource data and the design attributes and locations of PV systems. It combines these inputs with advanced algorithms to track cloud patterns to predict output.

The database includes locations of all PV systems in California. PV fleet power production was simulated using FleetView. Measured PV power production was provided by the CAISO. The measured data was used to identify performance issues and to compare with simulated results.

The PV fleet power production variability modeling results suggest that 3 percent Relative Mean Absolute Error (rMAE) can be achieved for PV fleet simulation for 15-minute time interval data over a six-week period given that accurate location-specific solar resource data is supplied; correct PV specifications are used; the PV simulation model is properly tuned; and PV plant operating status is reflected in the simulation to account for poor performance. Results also suggest that total error was over 7 percent if the model was not tuned and PV plant operating status was not reflected in the simulation.

The California Independent System Operator (CAISO) sees potential of using this approach in planning for system operations under alternative renewable energy scenarios. It also sees potential for using the approach for forecasting PV fleet production. Additional validation, however, is required before the method is usable by the CAISO to inform planning for future operational needs.

CHAPTER 1:
California PV System Database

PV fleet power prediction requires technical specifications for each PV system (see Figure 1). Thus, the first objective of this project is to develop a database of the PV systems in California.

Figure 1. Fleet simulation procedure.

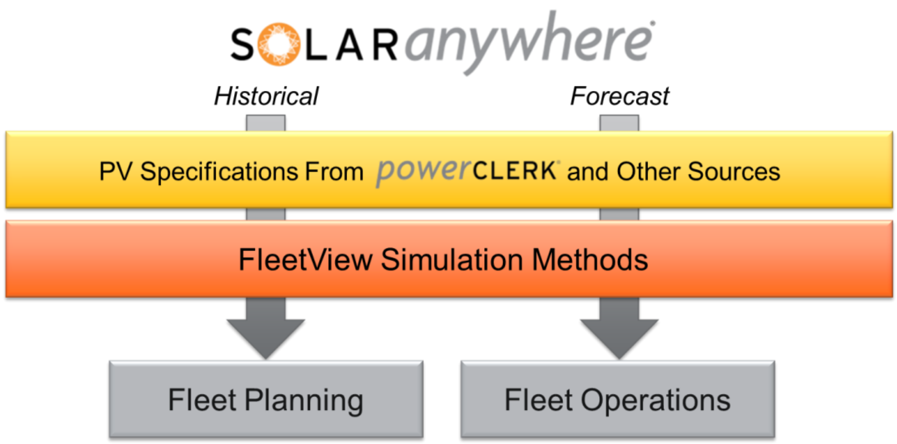

Many of the PV systems for California are included in CPR's PowerClerk® database. Some systems, such as the large PPA projects and systems installed by utilities without PowerClerk, are not included. The PowerClerk data set must therefore be supplemented by other data sources to provide the basis for fleet simulation. This section summarizes the PV hardware database that describes the grid-connected PV fleet in California.

1.1 Existing System Data in Database

The first step was to document and characterize the set of existing PV system data already in the PowerClerk database. This was accomplished by analyzing the PowerClerk set of programs. Table 1 summarizes the results at the beginning of this project (2010). It illustrates that the CSI programs at the California IOUs are well-covered, as are LADWP, SMUD, and the City of Palo Alto (CPAU) and a portion of Anaheim Public Utilities (APU).

Table 1: Existing PV Systems in PowerClerk

Program ID	Agency	Program	State	Obsolete	Number of Completed Applications
25	APU	Solar Electric Program	CA	FALSE	239
20	BWP	Burbank Water and Power Solar Support Program	CA	FALSE	72
11	CCSE	Small Commercial (< 10 kW) and All Residential	CA	FALSE	7,128
12	CCSE	Large Commercial (>= 10 kW)	CA	FALSE	86
28	CCSE	Multifamily Affordable Solar Housing	CA	FALSE	28
33	CPAU	PV Partners	CA	FALSE	14
50	LADWP	Solar Incentive Program	CA	FALSE	14
51	LADWP	Solar Incentive Program - Legacy	CA	FALSE	4,088
7	PG&E	Small Commercial (< 10 kW) and All Residential	CA	FALSE	30,668
8	PG&E	Large Commercial (>= 10 kW)	CA	FALSE	537
26	PG&E	Multifamily Affordable Solar Housing	CA	FALSE	57
9	SCE	Small Commercial (< 10 kW) and All Residential	CA	FALSE	15,601
10	SCE	Large Commercial (>= 10 kW)	CA	FALSE	249
27	SCE	Multifamily Affordable Solar Housing	CA	FALSE	29
4	SMUD	Residential Retrofit PV Program	CA	FALSE	1,099
18	SMUD	Commercial PV Program	CA	FALSE	69
19	SMUD	Commercial New Construction PV Program (Obsolete)	CA	TRUE	
34	SMUD	SMUD PV-Commercial	CA	FALSE	3
35	SMUD	SMUD Contracted-Residential Retrofit	CA	FALSE	343
36	SMUD	SMUD Contracted-Commercial	CA	FALSE	32
37	SMUD	Conversions-From SMUD to Customer Owned	CA	FALSE	81
38	SMUD	Community Solar	CA	FALSE	16
39	SMUD	SolarSmart	CA	FALSE	0
40	SMUD	SMUD Financed Church Program	CA	FALSE	15
41	SMUD	SMUD Contracted-Residential New Construction	CA	FALSE	110
42	SMUD	Residential PV-New Construction (pre SolarSmart)	CA	FALSE	139
43	SMUD	Commercial Self Install-No Rebate	CA	FALSE	11
44	SMUD	Residential Self Install-No Rebate	CA	FALSE	44
45	SMUD	SMUD PV-Utility	CA	FALSE	24
					60,796

1.2 Categories of Systems

The second step was to characterize the "missing" systems that would be the focus of the data collection effort. The main categories include:

- Renewable Portfolio Standard systems (RPS).
- Publicly owned utility Senate Bill-1 programs (POU SB-1).
- CEC's Emerging Renewables Program (ERP).
- New Solar Homes Partnership (NSHP).
- Single Family Affordable Solar Homes (SASH).
- Self-Generation Incentive Program (SGIP).

1.3 Data Collection Plan

The following describes the plan to collect, qualify and enter the data necessary to supplement the existing database. Sunterra Solar Inc., of Novato, California was selected as the contractor to research these systems and contact utilities as necessary to obtain system location, hardware and orientation details required for modeling.

The subcontractor performed the following services:

- Review the materials provided by CPR:
    - Sample Data Format.
    - List of Major Solar Projects.
    - List of California LSEs.
    - PV System Specification Sources.
- Contact utilities, project owners, and others by email and telephone to obtain PV system specifications.
- Enter data into a CPR-provided web-based database interface.
- Attend up to 3 face-to-face meetings in CPR's Napa office.

1.4 All California PV Database

Table 2 summarizes the data that was collected as of March 2012, now constituting the "All California PV Database." 78,025 of these systems (773 MW) existed in PowerClerk, primarily from the CSI program. RPS systems are large, multi-MW systems used by the IOUs (or owned by the IOUs) to meet state RPS obligations. This includes the 290 MW Agua Caliente project.

Table 2: Summary of the All-California PV Database at Start of Project

	No. Systems	Capacity (MW)
PowerClerk (existing)	78,025*	773
RPS	37	644
POU (SB-1)	45	50
CEC ERP (Before 2005)	11,455	45
CEC ERP (2005 and later)	16,602	78
New Solar Homes Partnership (NSHP)	12,543	40
Single Family Affordable Solar Homes (SASH)	1,949	7
Self-Generation Incentive Program (SGIP)	917	144
Total	**121,573**	**1,781**

Data from publicly-owned utilities (POUs) was obtained from the SB-1 reporting requirements. ERP, NSHP, SASH, and SGIP represent various incentive programs available to California consumers over several years. System-level data from each of these programs was obtained and included in the database.

Table 3 summarizes the data collected for the publicly owned utilities (POUs) based on required reporting under SB-1. The fleets were analyzed to prevent duplication in cases where the utility had systems described in PowerClerk.

Table 3: Publicly-Owned Utility Capacity (POU SB-1)

POU	Capacity (MW)
Alameda Municipal Power	0.60
Anaheim Public Utilities	1.97
Azusa Light & Water	0.15
Banning Public Utilities	0.73
Biggs Municipal Utilities	0.01
Burbank Water & Power	2.01
Colton Electric Utility	1.03
Glendale Water & Power	1.32
Gridley, City of	0.01
Healdsburg, City of	0.27
Hercules Municipal Utility	0.02
Imperial Irrigation District	4.06
Lassen Municipal Utility District	0.10
Lodi Electric Utility	1.20
Lompoc, City of	0.44
Merced Irrigation District	0.04
Modesto Irrigation District	9.01
Moreno Valley Electrical Utility	0.08
Needles, City of	0.07
Palo Alto, City of	2.73
Pasadena, Water & Power Department	3.22
Pittsburg Power Company	0.09
Plumas-Sierra Rural Electric Cooperative	0.19
Rancho Cucamonga Municipal Utility	0.06
Redding Electric Utility	0.63
Riverside Public Utilities	3.26
Roseville Electric	2.11
Santa Clara, City of	0.03
Shasta Lake, City of	0.05
Silicon Valley Power	4.94
Trinity Public Utility District	0.07
Truckee Donner Public Utilities District	0.27
Turlock Irrigation District	6.39
Ukiah, City of	0.08

1.5 Metered PV Fleet

Renewable Portfolio Standard (RPS) systems include large systems that utilities built or contracted to satisfy obligations. These systems are directly metered by the CAISO. These systems are also referred to as the metered systems, or the CAISO metered fleet.

The CAISO metered fleet consists of 46 PV plants. Forty-four of the plants are located in California. Two of the plants are located in Arizona and tie electrically to the CAISO's control area. Figure 2 summarizes the PV plant capacity (MW-AC) of the metered systems. Table 4 provides a list of the plants. The blue bars correspond to the ratings of each individual plant. The plants are ordered according to decreasing capacity. The red line presents cumulative PV plant capacity vs. the number of plants.

Figure 2: PV Plant Capacity and Cumulative Fleet Capacity vs. Number Metered Plants (MW-AC)

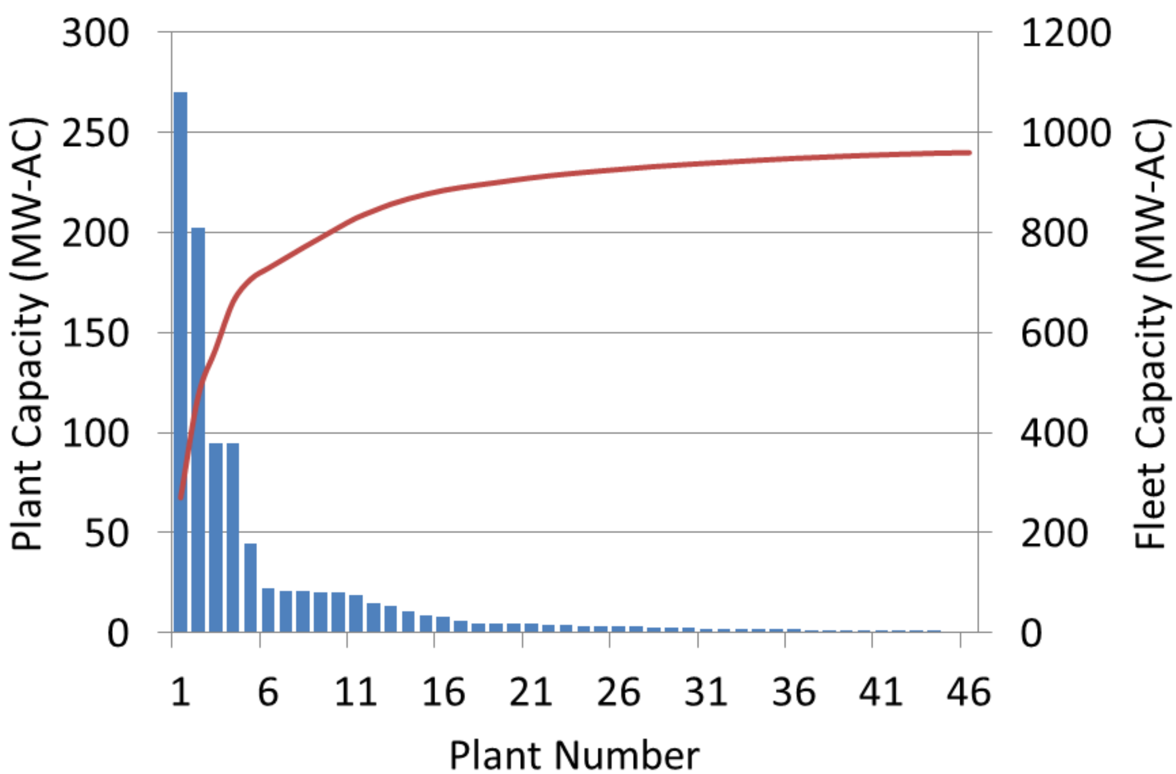

Table 4: List of Metered PV Plants

Plant Number	Capacity (MW-AC)
1	269.7
2	202.6
3	94.9
4	94.5
5	44.8
6	22.1
7	20.8
8	20.5
9	19.9
10	19.9
11	18.9
12	14.5
13	13.5
14	10.8
15	9.0
16	7.7
17	5.9
18	4.9
19	4.8
20	4.8
21	4.7
22	3.9
23	3.6

Plant Number	Capacity (MW-AC)
24	3.2
25	3.0
26	2.9
27	2.9
28	2.7
29	2.3
30	2.3
31	2.1
32	2.0
33	2.0
34	2.0
35	2.0
36	1.8
37	1.5
38	1.5
39	1.4
40	1.4
41	1.3
42	1.1
43	1.1
44	0.9
45	0.7
46	0.5

1.6 CAISO Control Area Groupings

CPR determined during the course of the project that it was insufficient to provide a single PV fleet prediction for the entire state of California. Rather, the CAISO required that PV fleet power predictions be grouped in specific ways. The CAISO specified that the data be grouped into five regions, as defined in Table 5.

In addition, the CAISO specified that PV systems need to be categorized as either metered systems or behind-the-meter systems for each region. Thus, ten PV fleet power predictions need to be provided to the CAISO.

Table 5: CAISO Regions

	Metered	Behind-the-Meter
PG&E Bay Area	✓	✓
PG&E Non-Bay Area	✓	✓
SCE Coastal	✓	✓
SCE Inland	✓	✓
SDG&E	✓	✓

After all of PV specifications were collected, each PV system was matched to one of the ten groups.

Figure 3 illustrates the mapping process for one PV system. Detailed PV specification data for a single system was mapped to the city of San Francisco. This, in turn, was mapped to the PG&E Bay Area CAISO region. Finally, it was a behind-the-meter PV system so it was mapped to the "PG&E Bay Area Behind-the-Meter" group.

This process was repeated for all metered and behind-the-meter PV systems. The resulting capacity as of January 1, 2013 for the state of California is presented in Figure 4. In addition, the PV systems that supplied power to other control areas were mapped to their respective control areas.

Figure 3: PV System Mapping Process

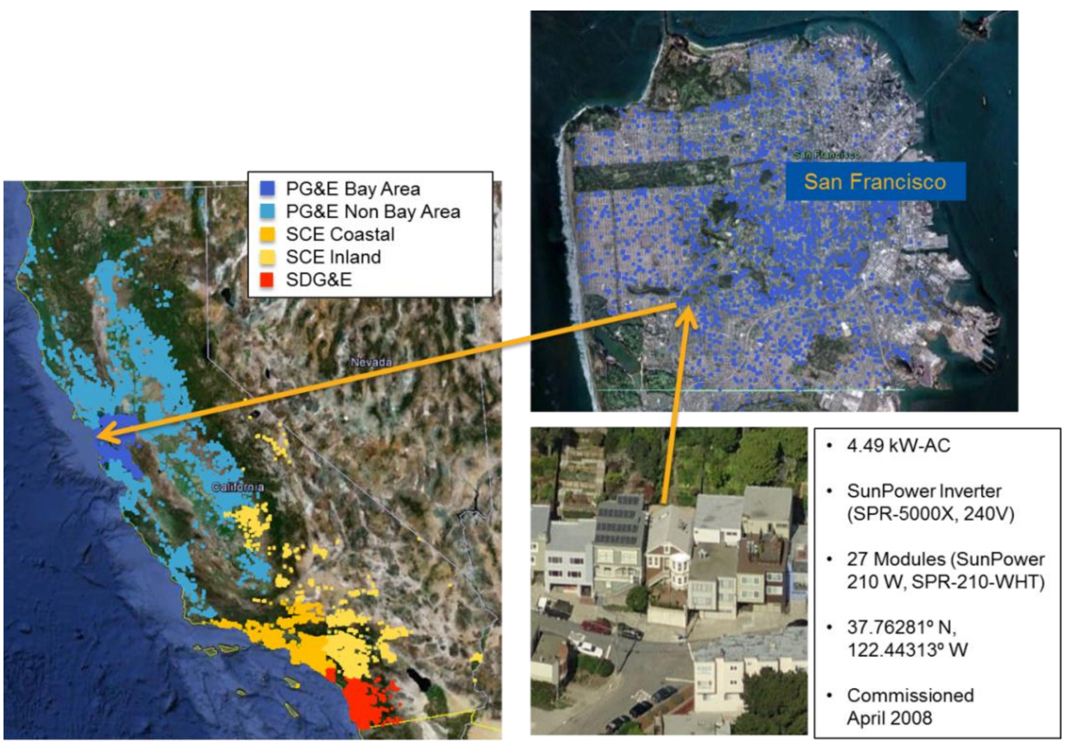

Figure 4: California PV Capacity

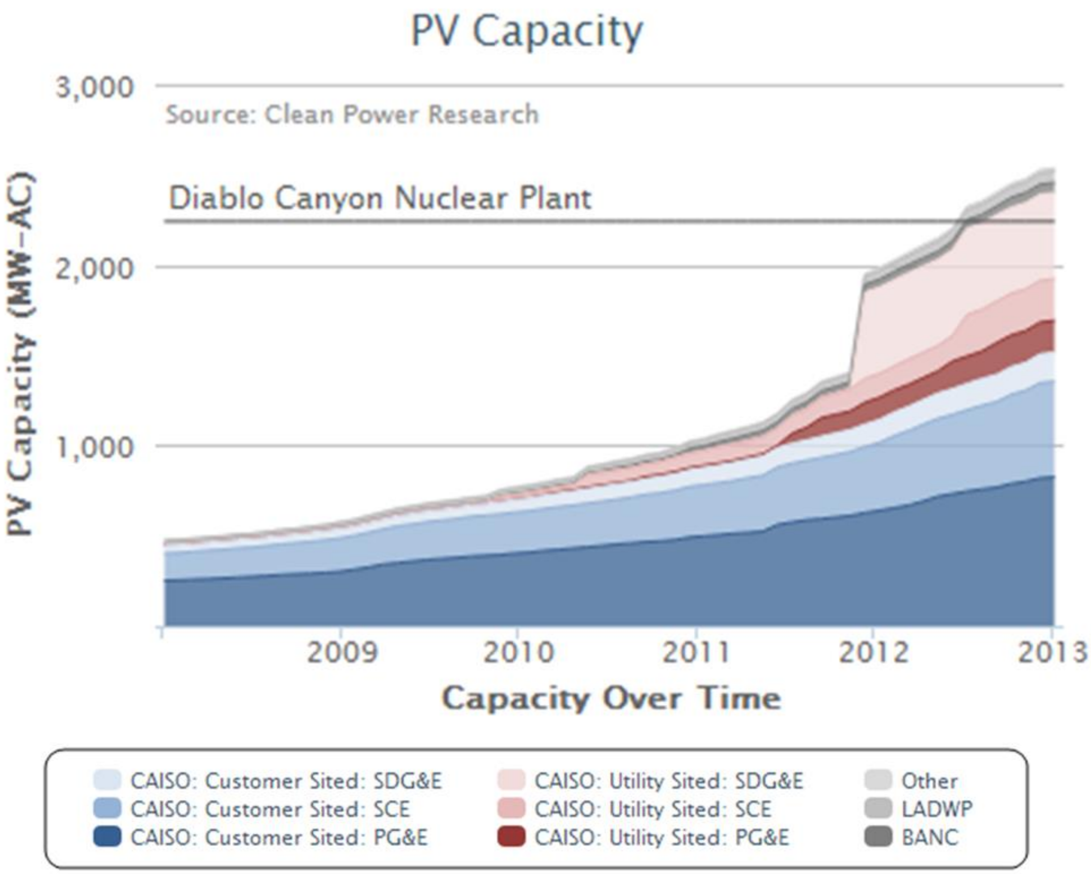

Chapter 2: High Resolution Solar Resource Data

PV fleet power prediction requires solar resource data that corresponds to the location of each PV system (see Figure 1). The second task of this project was to assess high resolution solar data accuracy for a defined fleet of PV systems.

2.1 Definitions

It is important to clearly define what is meant by accuracy before discussing solar resource data accuracy. Accuracy validation often means different things to different people. As such, it is useful to begin with a definition of how accuracy quantification can be performed.

Three fundamental questions need to be answered to provide a clear definition of how accuracy quantification is performed.

1. What is the data source?
2. What are the time attributes?
3. What is the evaluation metric?

2.1.1 Data Source

The first step is to identify the data that is being evaluated. Options include irradiance data or simulated PV power production using irradiance data and other parameters. In addition, the analysis can be performed for individual locations or fleets (i.e., multiple locations). This chapter focuses on irradiance data. The analysis is performed for both individual locations and fleets. A subsequent chapter assesses accuracy for PV fleet production data.

2.1.2 Time Attributes

The second step is to specify the required time attributes. These include:

- **Time period**: total amount of data included in the analysis. This can range from a few minutes to many years. This chapter focuses on one year worth of data.
- **Time interval**: how the data in the time period is binned. This can range from a few seconds to annually. For example, if the time period is one year and the time interval is one hour, the time period would be binned into 8,760 time increments. This chapter examines one-minute to one-year time intervals.
- **Time perspective**: when the predicted observation is reported. This can range from historical (backward looking) to forecasted a few hours ahead to forecasted multiple days ahead (forward looking). This chapter focuses on historical data.

2.1.3 Evaluation Metric

The third step is to select the evaluation metric. Error quantification metrics used in assessing absolute irradiance model accuracy such as Root Mean Square Error (RMSE) and Mean Absolute Error (MAE) have been precisely defined [17], [18]. Their relative counterpart (results expressed in percent), however, can be subject to interpretation and may cover a wide range of values for a given set of data depending on reporting practice.

Appendix A suggests that the MAE relative to available energy (rMAE) is a good method to measure relative dispersion error. This is the method used in the present analysis. The MAE relative to the average energy available is calculated by summing the absolute error for each time interval over the time period, and then dividing by the total available energy.

$$Relative\ Mean\ Abosolute\ Error = \frac{\sum_{t=1}^{N}\left|I_t^{test} - I_t^{ref}\right|}{\sum_{t=1}^{N} I_t^{ref}} \qquad (1)$$

where I_t^{test} is the test irradiance at time t, I_t^{ref} is the reference irradiance at time t, and N is the number of time intervals.

It is useful to provide a hypothetical example of how to calculate the rMAE. A short time period (one day) is selected in order to graphically illustrate the calculations; the actual calculations in this paper use a one year time period.

As presented in Figure 5, the process is follows:

- Select time period: 1 day.
- Select time interval: 1 hour.
- Calculate absolute error for each hour and sum the result as described in the top part of Equation (1): 1.6 kWh/m²/day.
- Calculate available energy for each hour from reference data and sum the result as described in the bottom part of Equation (1): 4.5 kWh/m²/day.
- Calculate Relative Mean Absolute Error: 36% (i.e., 1.6/4.5).

Figure 5: Mean Absolute Error Relative to Available Energy Calculation Example

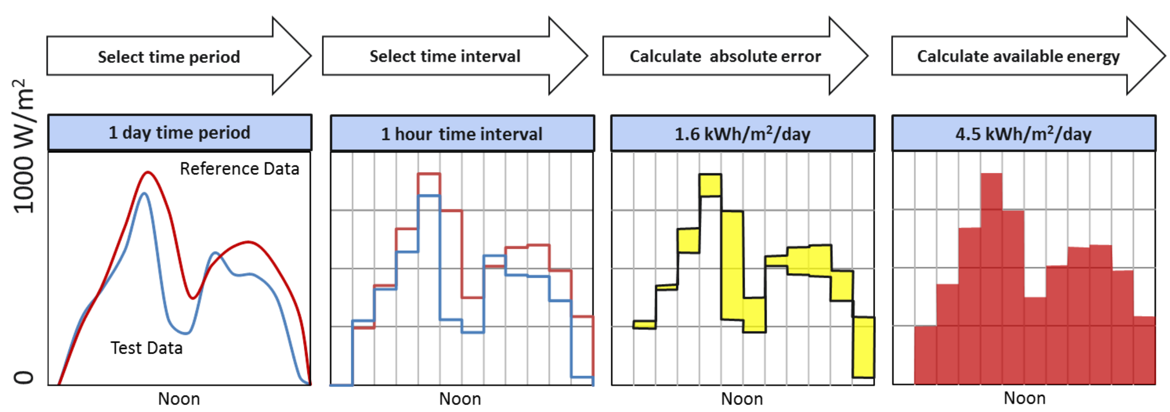

It is important to note that a more often reported measurement of error is MAE relative to generating capacity. In the above example, however, it is unclear over what time period the generating capacity should be selected. Should it be capacity during daylight hours or capacity over the entire day, including night time hours? MAE relative to daytime capacity is about 13.3% (i.e., 1.6/12) while Mean Absolute Error relative to full day capacity is about 6.6% (i.e., 1.6/24).

It is due to this sort of ambiguity, as well as the fact that MAE relative to energy is a much more stringent metric (e.g., in this example, MAE relative to energy is 6 times higher than MAE relative to daily generation capacity), that the MAE relative to energy (rMAE) is selected as the evaluation metric.

2.2 Approach

This metric can be used to quantify irradiance data accuracy for a one-year time period (2011) with time intervals ranging from one-minute to one-year using a historical time perspective. The analysis was performed for both individual locations and the ensemble of those locations.

2.3 Location Selection

2.3.1 Locations Selected for Validation

Ten of the 46 metered locations were randomly selected for validation purposes. In order to perform the detailed analysis, each location had to have two global horizontal insolation (GHI) monitoring devices available on site and have one year's (2011) worth of data available. There were six locations that passed this initial screening.

A total of six test locations were analyzed where PV systems are located within the CAISO control area. The locations are identified as locations A through F. Each location is equipped with two redundant global horizontal irradiance (GHI) sensors. One of the sensors was used as a reference and compared to four test configurations: the second ground sensor, and three satellite-derived sources (SolarAnywhere Standard, Enhanced, and High Resolution data sets).

The validation approach involved the following steps:

- Obtain time-series GHI data for 2011 for six locations:
    - 4-second data averaged into 1-minute time intervals from two separate sensors at each location (sources: CAISO [20])
    - Satellite based data at the following resolutions (source: SolarAnywhere [14])
        - 1 minute, 1 km grid (High Resolution)
        - ½ hour, 1 km grid (Enhanced Resolution)
        - 1 hour, 10 km grid (Standard Resolution)
- Time-synchronize data sets by converting ground sensor data from Pacific Daylight Time to Pacific Standard Time.
- Evaluate all observations for data quality; exclude data where any one of the data sources has data quality issues.
- Calculate rMAE using the ground sensor that minimizes SolarAnywhere error as a reference.
- Calculate rMAE using the other ground sensor as a reference.
- Repeat the analysis for fleets of locations.

2.3.2 Obtain Time Series Data

CPR extended SolarAnywhere Standard Resolution (10 km spatial/1 hour temporal resolution) to SolarAnywhere Enhanced Resolution (1 km spatial/ 30 minute temporal resolution) under a previous contract.[1] Figure 6 illustrates the increase in resolution for San Francisco, CA.

Figure 6: SolarAnywhere Standard and Enhanced Resolution

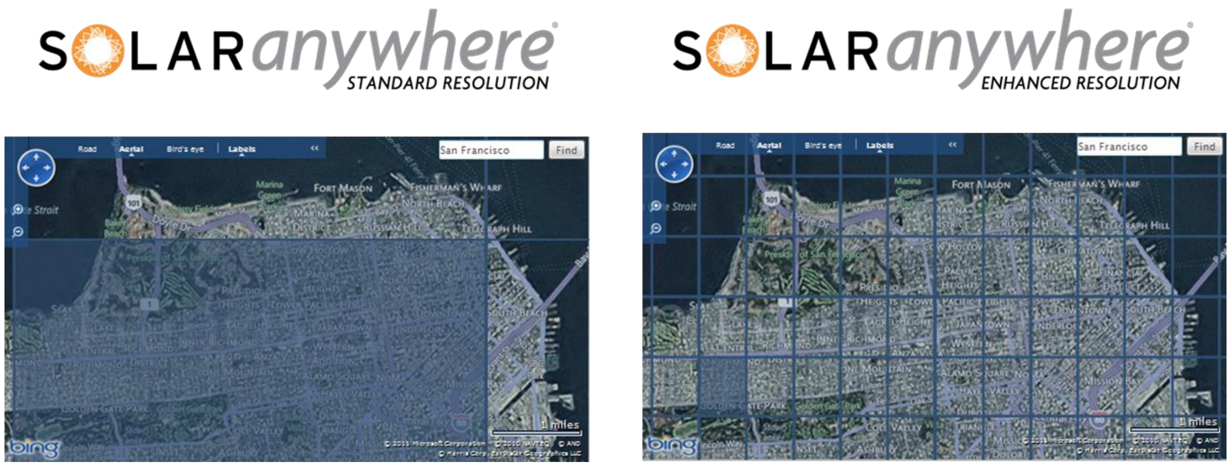

(San Francisco, CA)

A critical part of this CEC project was to extend SolarAnywhere Enhanced Resolution to SolarAnywhere High Resolution (1 km spatial/ 1 minute temporal resolution). The data was generated for all selected locations. Figure 7 presents a sample of the data for one day (July 4, 2011) at one location (CAISO Site A).

[1] California Solar Initiative Solicitation #1 Grant Agreement, "Advanced Modeling and Verification for High Penetration PV".

Figure 7: Time Series Data for All Data Sources on July 4, 2011 at CAISO Site A

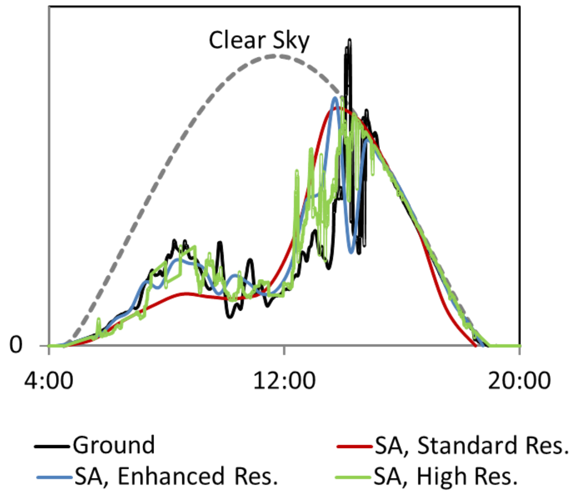

Note: only one ground source is shown for clarity purposes

2.3.3 Evaluate All Observations for Data Quality

As mentioned above, one of the steps in the analysis was to evaluate all observations for data quality. When evaluating accuracy, it is often simply assumed that reference data is correct. This assumption is made due to the difficulty in determining whether or not the reference data is correct: to what can the reference data be compared?

A unique aspect of the data provided by the CAISO is that all the locations have two ground sensors. As a result, since either sensor could be the reference, the data quality of the ground sensors was assessed by comparing the two ground data sets.

This was the process used to assess data quality:

(1) Compare the two sets of ground sensor data to each other to determine when one value is substantially different than the other value.
(2) Compare the enhanced resolution satellite and ground sensor data to search for 0 values occurring at incorrect times (e.g., mid-day on otherwise clear day) to determine when the satellite data is invalid.
(3) Compare ground sensor data to the SolarAnywhere Enhanced Res. data to determine if both ground observations are the same but are obviously incorrect (e.g., the irradiance value remains at a constant level for many hours).

The complete data set was evaluated and then potential outliers were manually evaluated and screened for each of these steps. Figure 8 illustrates the screening result when comparing the two ground sensors at one location. All of the data points would lie on the 45 degree red line if they were identical. The blue symbols correspond to valid data and the black symbols correspond to invalid data. Figure 9 illustrates the issue for one of the invalid observations when one of the sensor's recorded values remained constant after solar noon. Figure 10 illustrates the case when both ground sensors produced a similar value but were obviously incorrect, reading a constant low value on an otherwise clear day as assessed from the satellite data. Figure 11 illustrates the case when there was a night-time calibration error across the year. Site E was missing more than a month of data during the first part of the year as well as a five percent difference between the two ground sensors.

Sites E and F were eliminated from the analysis as a result of the data filtering process. The remaining sites had about one percent of the ground data marked as invalid.

Figure 8: Half-Hour Energy Production in 2011 from Meter 2 vs. Meter 1 (Site A)

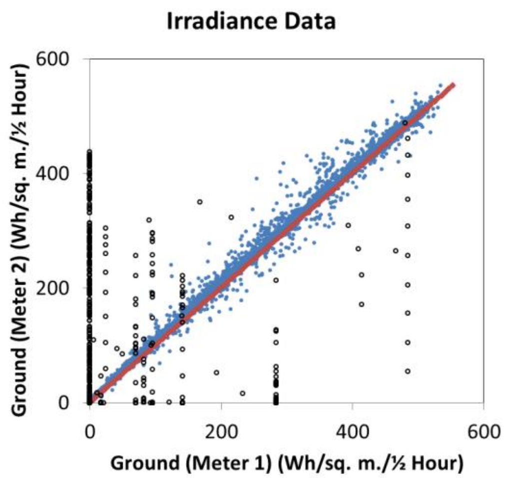

Figure 9: Example of When Only One of the Ground Sensors Has Invalid Data

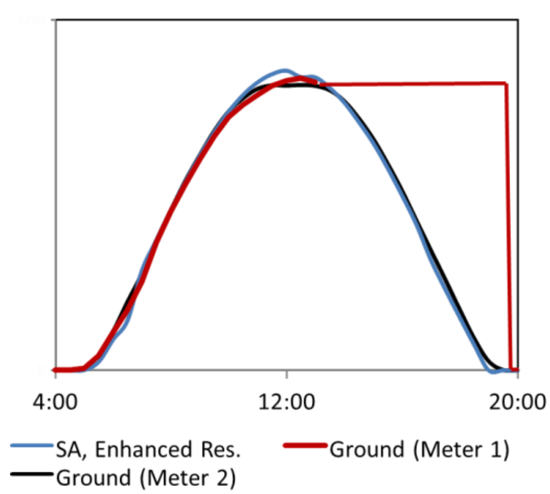

(Site A, June 22, 2011)

Figure 10: Example of When Both Ground Sensors Have Invalid Data

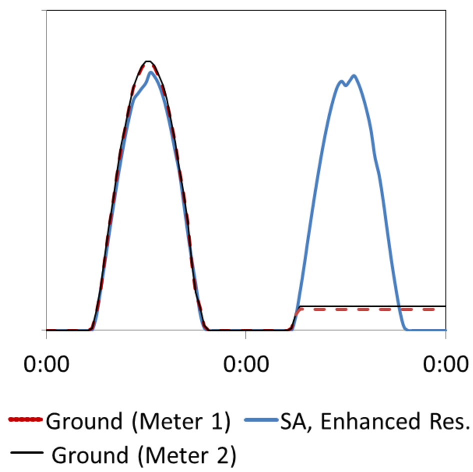

(Site C, May 1-2, 2011)

Figure 11: Site F Has a Night-Time Calibration Error across the Year

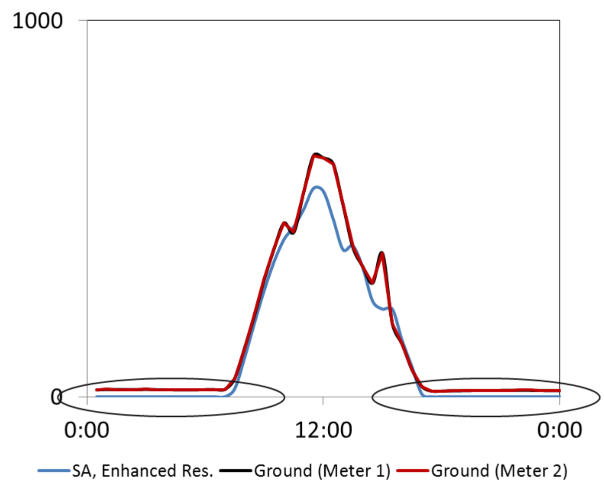

2.4 Results

rMAE was calculated for three scenarios:

- Each location individually.
- Average of individual locations.
- Fleet of locations.

2.4.1 Each Individual Location

Figure 12 presents the rMAE for each of the four locations using time intervals ranging from 1 minute to 1 year.

Figure 12: Relative MAE for Each Location Individually

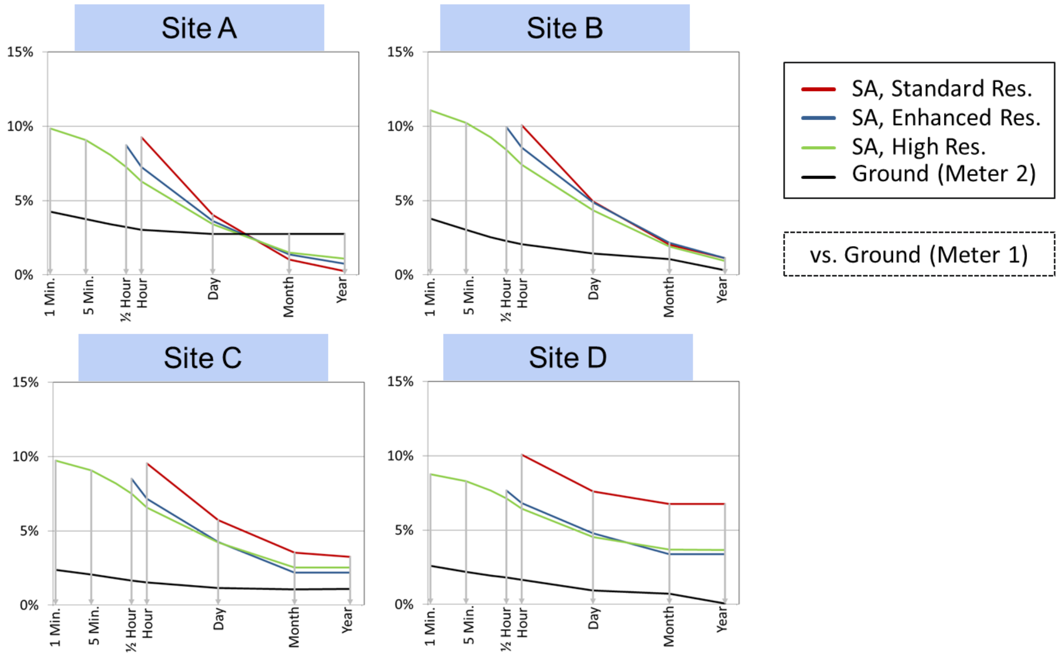

2.4.2 Average of Individual Locations

Figure 13 presents the average rMAE of four individual locations. The black line summarizes the error when two ground stations were used (one was the reference and the other was the test). The green, blue, and red regions summarize the error when SolarAnywhere High, Standard, and Enhanced Resolution were compared to the ground sensor. The green, blue, and red areas are regions rather than lines because they compare satellite data to ground data using the two different ground sensors: the top of the region is the comparison using the ground sensor that maximizes error; the bottom of the region is the comparison using the ground sensor that minimizes error.

There are several important things to notice in the figure. First, as expected, error decreases for all data sources as the time interval increases. Second, accuracy improves for each of the three satellite models as the spatial and temporal resolutions are increased. Third, error exists even between two ground sensors that are in almost the same location (i.e., ground sensors have 1 percent annual error). Fourth, SolarAnywhere High Resolution has only 10 percent error over a one minute time interval, 7 percent error over a one hour time interval, and 2 to 3 percent error on a one year time interval.

Figure 13: Average MAE of 4 Individual Locations

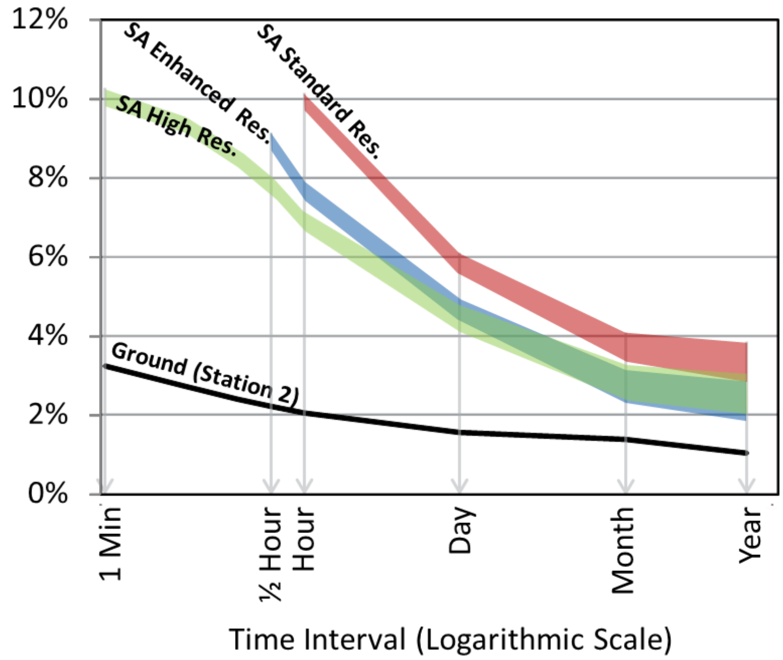

2.4.3 Fleet of Locations

As illustrated by the list of References, a number of studies have examined the issue of PV output variability. A consistent finding of these studies is that variability is reduced when PV systems are geographically dispersed. That is, variability is reduced as the number of systems increases across a sufficiently large geographic region.

So far, this report has focused on the error associated with individual locations. While individual locations are of interest in some cases, there are certainly many other cases in the utility industry when users are most interested in the error associated with a set of locations.

The rMAE analysis was repeated with the input data being the combined irradiance across four locations. The results are presented in Figure 14. A clear reduction in error due to combining locations can be seen by comparing Figure 14 to Figure 13. That is, the effect of geographic dispersion on reducing output variability reduction that has been observed by others is now also observed with regard to prediction accuracy: accuracy improves as a geographically diverse set of independent locations are combined.

Figure 14: MAE of 4 Locations Combined

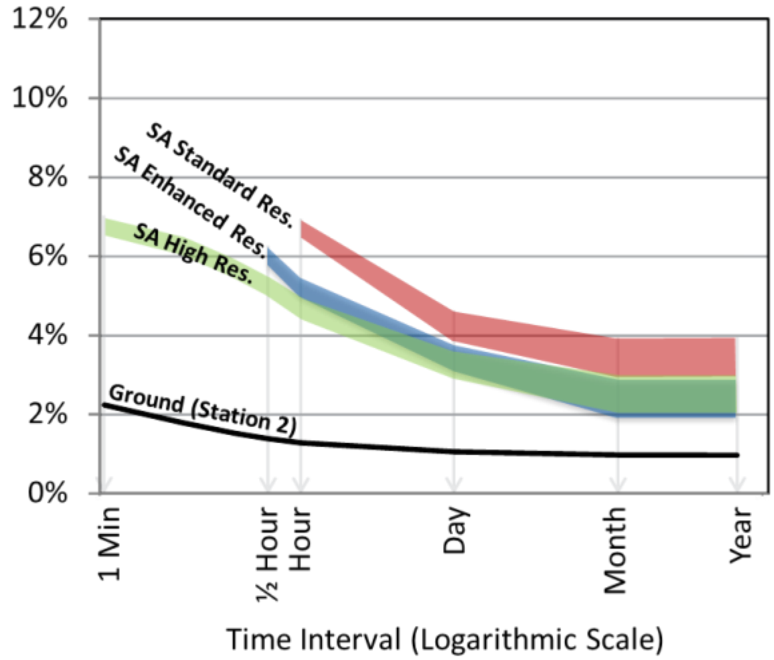

In order to demonstrate why this is occurring, a "worst day" analysis was performed. In particular, the "worst day of the year was selected (i.e., the day that had the highest MAE calculated using a one-day time period and one-minute time interval for any of the four locations). The results are illustrated in Figure 15. The top graph in the figure is a probability distribution of the daily MAE for all 4 sites and 365 days per year. As can be seen in the figure, the worst day of the year had 103 percent daily rMAE on a one minute basis.

The black line in the figure points to the graph of the one minute GHI for January 30, 2011, at Site B, the worst day and worst site of the year. SolarAnywhere High Resolution clearly over predicted irradiance on this day. The prediction at the other three sites, however, was good. As a result, the combined error for the day is 33 percent. As shown by the red line in the top distribution figure, this was still the day that had the highest daily error, but it is much lower than the one site by itself.

Figure 15: Worst Day, Worst Site Analysis.

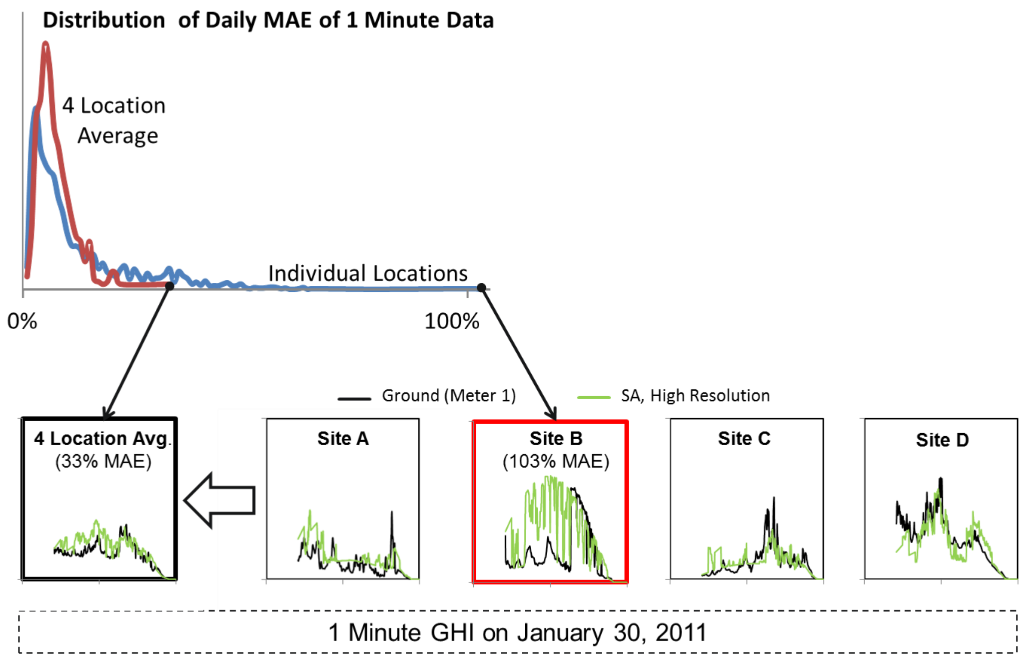

Site B Had Highest Daily Error on Jan. 30, 2011.
The 4 Location Average Reduces Effect.

Furthermore, fleet error appears to be able to be approximated from average individual location error as follows.

$$Predicted\ Mean\ Abosolute\ Error = \frac{\mathrm{E}[MAE\ for\ selected\ time\ interval]}{\sqrt{N}} + |\mathrm{E}[MBE]|\left(1 - \frac{1}{\sqrt{N}}\right) \quad (2)$$

where E[] is the expected value, MBE is the mean bias error, and N is the number of independent locations. This proposed relationship will have to be ascertained with a larger sample of data points, but it can be stated that the $\sqrt{N}$ dependence is an inference of the reasonable assumptions that errors at individual locations are not correlated. This follows along the Strong Law of Large Numbers that states that the average of a sequence of independent random variables having a common distribution will, with probability 1, converge to the mean of that distribution as the number of observations goes infinity [21].

2.5 Summary

Results suggest that, first, satellite-based irradiance has annual error comparable to ground sensors. Thus, satellite data may perform as well as ground data for plant siting at a fraction of the cost plus the benefit of long-term data streams. It should be noted that ground sensors, even well maintained, produce considerably more invalid data points than the satellite (a ratio of one hundred to one in the present study), and that the satellite data were key in detecting these erroneous data points (particularly when both redundant sensors were inaccurate at the same time).

Second, high resolution satellite-based irradiance has 10 percent one minute error for a single location, making it suited to provide the basis for data required to perform high penetration PV studies.

Third, accuracy improves predictably due to the benefit of geographic dispersion. That is, the effect of geographic dispersion on reducing output variability reduction that has been observed by others is now also observed with regard to prediction accuracy.

Chapter 3:
PV Fleet Simulation

3.1 Introduction

This chapter describes how to generate time series PV fleet production data for consumption by CAISO processes. This required the following:

- Interact with the CAISO to develop a data format specification for time series PV fleet data that will be compatible with their system expectations.
- Design, test, and implement a method to produce a set of synthetic PV fleet performance data.
- Create time series data streams, deliver to the CAISO for their use, and assist the CAISO in analyzing, using, and implementing this data as required.

3.2 Forecast Requirements

The first step of the process was to interact with the CAISO to develop data format specifications for time series PV fleet data that will be compatible with their system expectations. The CAISO and CPR met on several occasions to finalize this information. Table 6 and Table 7 present the CAISO's near-term and long-term requirements. The requirements are classified according to the Real-Time Power Dispatch (RTPD) market and the Day-Ahead market.

The requirements specified how often the forecasts needed to be updated, when the forecasts were due, forecast time interval, forecast time horizon, and whether or not the forecasts should include uncertainty bounds (i.e., confidence intervals). The goal under this project is to satisfy the CAISO's near-term requirements. Subsequent work will satisfy their long-term requirements.

Table 6: Near-Term CAISO Requirements

Market	Update Frequency	Forecast Due	Forecast Interval	Forecast Horizon	Include Uncertainty?
Real-Time Power Dispatch	30 min	Every 30 minutes	15 min	12 hours	No
Day-Ahead	Daily	7:45 am of day before	1 hour	6 days	No

Table 7: Long-Term CAISO Requirements

Market	Update Frequency	Forecast Due	Forecast Interval	Forecast Horizon	Include Uncertainty?
Real-Time Power Dispatch	15 min	Every 15 minutes	15 min	12 hours	Yes
Day-Ahead	Hourly	45 min past hour	1 hour	6 days	Yes

3.3 PV Fleet Simulation Method

The second step was to design, test, and implement a method to simulate PV fleet performance data per the CAISO's requirements listed in Table 6. Three components are required to simulate PV fleet power production (as illustrated in **Error! Reference source not found.**):

1. Solar resource data.
2. PV plant specification data.
3. PV fleet simulation model.

3.3.1 Solar Resource Data

The first component that is required to simulate PV fleet power production is the solar resource data. The SolarAnywhere Enhanced Resolution data is used for the simulation for all of the plants in California. This database consists of solar resource observations produced every 30 minutes based on satellite imagery for the state of California using a 1 km grid. Higher speed data observations are generated using these native images using a cloud motion vector interpolation approach. The cloud motion vector approach takes two consecutive images and infers cloud movement (i.e., speed and direction) based on a comparison of the two images.

The SolarAnywhere Standard Resolution data is used for the simulation for the plants in Arizona. This database consists of solar resource observations produced every 60 minutes based on satellite imagery using a 10 km grid.

Details of the solar resource data are described above.

3.3.2 PV Plant Specification Data

The second component that is required to simulate PV fleet power production is a set of PV system specifications. PV systems in California can broadly be categorized as being either metered or behind-the-meter. The key is which systems should be included.

Validating simulated vs. measured data requires that measured data is available. As a result, the metered systems provide the basis for validation efforts. An earlier chapter described how the CAISO metered fleet consists of 46 PV plants. It also presented the capacity (MW-AC) of each system. The total capacity of this fleet is 959 MW-AC.

Details of this data collection effort are described above.

3.3.3 PV Fleet Simulation Model

The third component that is required to simulate PV fleet power production is a PV fleet simulation model. SolarAnywhere® FleetView™ is used for this task.

One approach to simulating PV fleet output is to calculate average irradiance across the fleet and average capacity of the fleet and then to perform a single simulation. This approach, however, fails to capture the weather variability associated with specific locations because it artificially smooths fleet output.

FleetView takes a much more detailed approach. Power production is simulated for every PV plant independently. The simulations from the individual plants are then summed to obtain fleet production. This approach captures site-specific resource variability.

3.3.4 Rapid Calculations

In addition to having three requirements to be able to produce the fleet predictions, the calculations need to be performed at a speed that satisfied the CAISO requirements. The SolarAnywhere FleetView software service was initially designed to provide forecast data across large geographic areas for a limited number of PV systems. The CAISO, however, required forecast data every 30 minutes for a large number of PV systems (currently at 130,000 systems). As a result, the method of producing and delivering the data needed to be modified to accommodate the CAISO's requirements.

Two broad categories of modifications were required. One category was to identify inefficiencies in existing solar resource forecast software code and to implement code changes to speed processing. Another category was to migrate SolarAnywhere software solution from a single server application to a multi-server, cloud-based application. This was required in order to make the forecasting process scalable according to the number of PV systems.

It initially required more than 30 minutes to produce forecasts. This was an issue because the CAISO needed a forecast every 30 minutes, but the forecast could not be completed in less than 30 minutes. The forecast production time has now been reduced to less than 30 minutes.

3.4 Time Series Data

The next step was to create time series data streams, deliver the data to the CAISO for their use, and assist the CAISO in analyzing, using, and implementing this data as required. CPR began producing forecasts and posting them to a secure FTP site in January, 2013. CPR went through several months of testing to ensure that the data was reliably delivered. The CAISO has initiated the process of downloading the data.

An Excel file is posted to the secure FTP site every half hour for the RTPD market. A file is posted every day for the Day-Ahead market. Each file contains three columns: Period Ending, Region, and Power (MW). Figure 16 presents the first several rows in an RTPD file that was produced on 5/9/2013 at 10:30.

Figure 16: Sample RTPD PV Fleet Forecast File

	A	B	C
1	**Period Ending**	**Region**	**Power (MW)**
2	5/9/2013 10:45	Non-Metered: PG&E Bay Area	147.3
3	5/9/2013 11:00	Non-Metered: PG&E Bay Area	151.7
4	5/9/2013 11:15	Non-Metered: PG&E Bay Area	156.0
5	5/9/2013 11:30	Non-Metered: PG&E Bay Area	159.3
6	5/9/2013 11:45	Non-Metered: PG&E Bay Area	162.6
7	5/9/2013 12:00	Non-Metered: PG&E Bay Area	163.1
8	5/9/2013 12:15	Non-Metered: PG&E Bay Area	163.5
9	5/9/2013 12:30	Non-Metered: PG&E Bay Area	164.0
10	5/9/2013 12:45	Non-Metered: PG&E Bay Area	164.5
11	5/9/2013 13:00	Non-Metered: PG&E Bay Area	167.0
12	5/9/2013 13:15	Non-Metered: PG&E Bay Area	169.6
13	5/9/2013 13:30	Non-Metered: PG&E Bay Area	191.7

3.5 Summary

This chapter described how CPR is providing time series PV fleet production data for the CAISO. This included interacting with the CAISO to determine forecast data requirements, modifying the PV fleet power production simulation method in SolarAnywhere FleetView to accommodate these requirements, and creating the time series data. The next chapter validates simulated PV fleet power production in comparison to measured data provided by the CAISO.

Chapter 4: PV Fleet Simulation Validation

4.1 Introduction

This chapter describes the validation of simulated PV fleet production using measured data provided by the CAISO. This required the following:

- Work with the CAISO to determine data availability, resolve time synchronization issues, and take steps necessary to ensure data integrity.
- Obtain data and upload to the contractor's data servers.
- Perform analysis using methods previously used for similar United States data sources.

4.2 Approach

Validation requires simulated and measured data. The previous chapter discussed how the data was simulated using FleetView. The measured data was provided by the CAISO. The CAISO measures power production every four seconds for 46 PV plants. A 15-minute time interval is critical to the CAISO's forecasting efforts above. Thus, the four-second measured PV power production was averaged to 15-minute data.

4.3 Results

4.3.1 Sources of Error

Inaccuracies degrade the ability of the simulation to reflect measured performance. These inaccuracies can be grouped into three categories.

1. Solar resource.
2. PV modeling.
3. PV plant performance issues.

Solar resource inaccuracies include errors in historical or forecasted solar resource data. PV modeling inaccuracies refer to limitations in the PV fleet modeling algorithms. PV plant performance issues reflect errors that occur because the plant is not operating as expected.

The effects of solar resource and PV modeling inaccuracies are fairly obvious. Inaccurate solar resource data (historical or forecasted) and/or PV fleet modeling algorithms clearly limit the simulation's ability to reflect measured performance.

PV plant performance issues are more subtle. Differences between simulated and measured PV production can still occur even if the simulation method perfectly predicts measured PV fleet power production for a fleet that is operating perfectly. Differences can occur if the actual PV fleet does not operate as expected due to system performance issues. That is, inaccuracies can occur that are unrelated to the fundamental simulation methodology. They are related to lack of incorporation of poor performance into the simulation.

4.3.2 PV Plant Performance Issues

The first step of the evaluation, therefore, is to determine how to address PV performance issues. One option is to incorporate plant status into the simulation methodology. The simulation, for example, would reflect a capacity reduction if a plant was only operating at 50 percent capacity. This option requires obtaining PV plant status information. This information, unfortunately, was unavailable for the CAISO fleet of PV systems.

An alternative approach is to identify days when the individual plants had sub-par performance. These days and plants are then eliminated from the fleet simulation. This is the approach that was taken for this project.

Fifteen-minute measured and simulated data were obtained for 46 CAISO metered PV plants from March 10, 2013 to April 19, 2013. The time series data were compared for each of the plants individually. The data was visually examined to assess days when the PV plant was either not operating or was clearly underperforming. Figure 17 and Figure 18 present the results of the analysis for two of the 46 plants. The red and blue lines correspond to simulated and measured data. The shaded areas represent days with plant performance issues. The dashed line corresponds to the daily rMAE. Figure 17 corresponds to a plant that operated well during the whole time period. Figure 18 corresponds to a plant that had significant operational issues.

Figure 17: Example of PV Plant that Operated as Expected

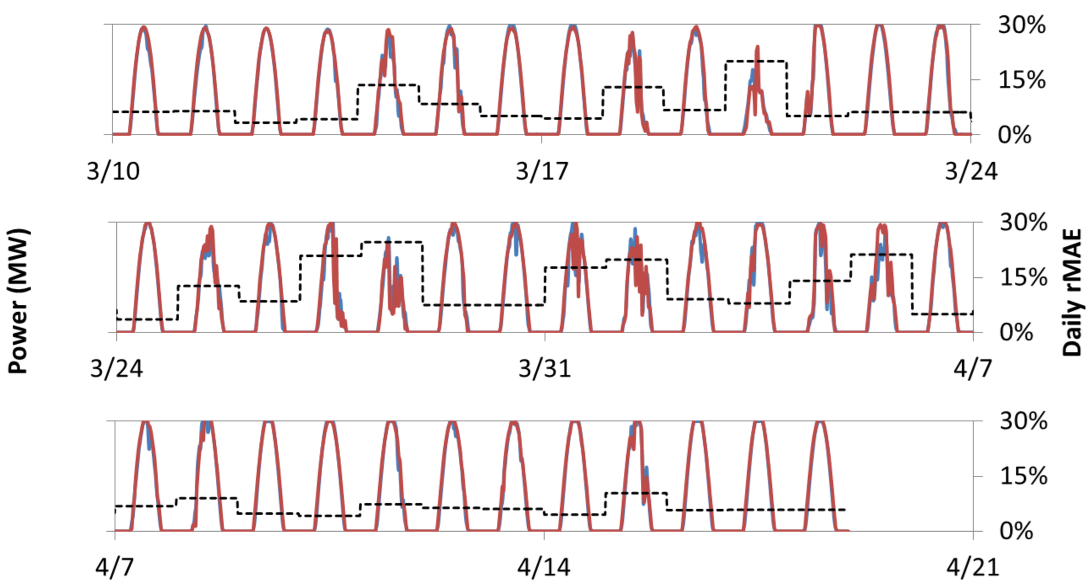

Figure 18: Example of PV Plant with Possible Performance Issues

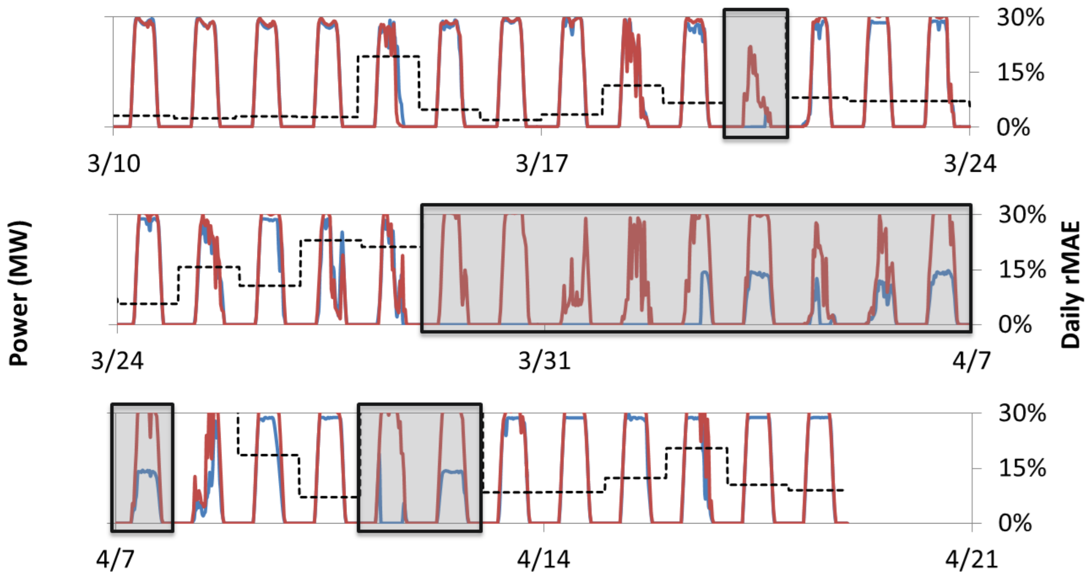

This process was repeated for all of the plants. Figure 19 summarizes plant performance for all 46 plants. The y-axis corresponds to the plant number and the x-axis corresponds to the date. Blue corresponds to normal operation and red corresponds to performance issues. The figure suggests that the PV fleet experienced a significant number of performance issues over the six-week analysis period.

Figure 19: Summary of Performance Issues for All Metered Plants

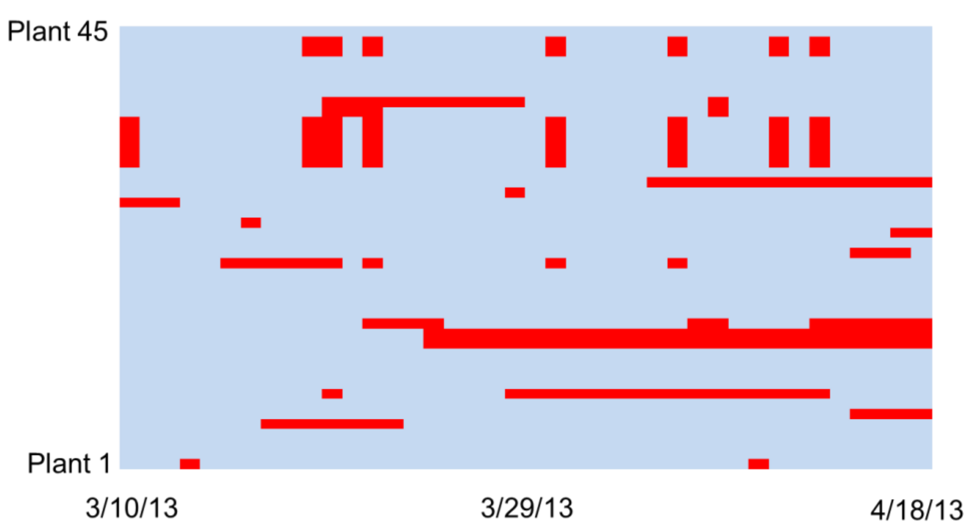

4.3.3 PV Fleet Simulations

4.3.3.1 Time Series Data

Simulations were performed using FleetView with and without plant filtering results from the previous section. Figure 20 presents PV fleet output without filtering. Figure 21 presents PV fleet output with filtering. A comparison of the two figures illustrates the improvement in accuracy by taking PV plant performance issues into consideration.

Figure 20: PV Fleet Production before PV Performance Filtering

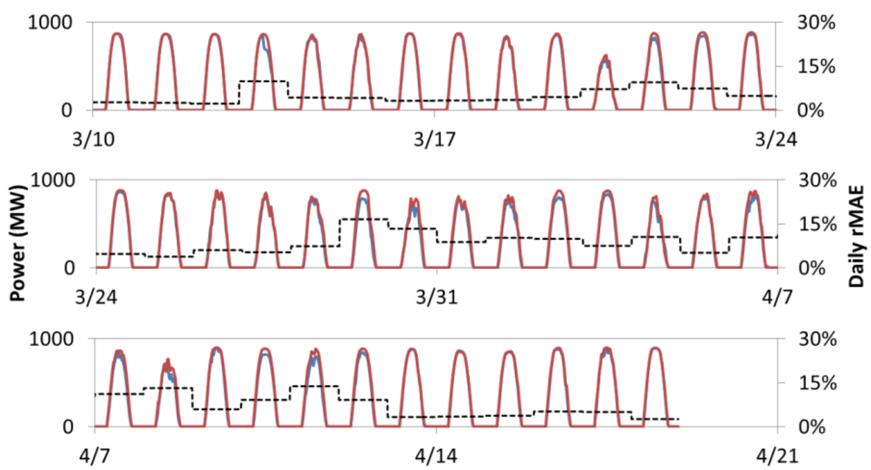

Figure 21: PV Fleet Production after PV Performance Filtering

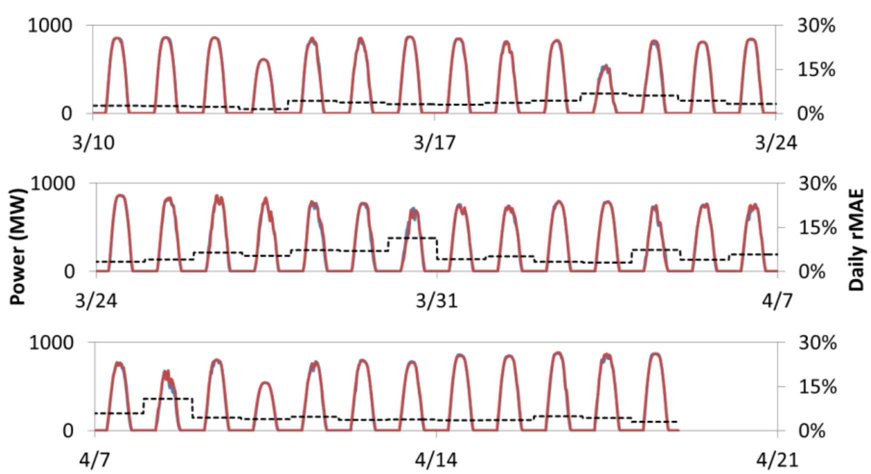

4.3.3.2 Simulated vs. Measured Data

An alternative way to present the data in Figure 20 is to plot simulated vs. measured average power for each 15-minute interval. Figure 22 presents the data in this manner. All of the blue markers would be on the red line if simulated and measured results matched perfectly. The top of the figure corresponds to the "Initial" case of PV fleet output without PV performance filtering (it corresponds to Figure 20). A consistent power-related bias can be observed.

This bias can be reduced by applying the tuning curve presented in Figure 23. The "Tuned" case is presented in the center of Figure 22. Significant scatter, however, can still be observed. This can be reduced by filtering the data for PV performance using the filtering from the previous section.

The "Tuned & Filtered" case is presented in the bottom of Figure 22. There is a good alignment between simulated and measured data after making the tuning and filtering adjustments.

Figure 22: Simulated vs. Measured Average 15-Minute Power for CAISO Metered PV Fleet

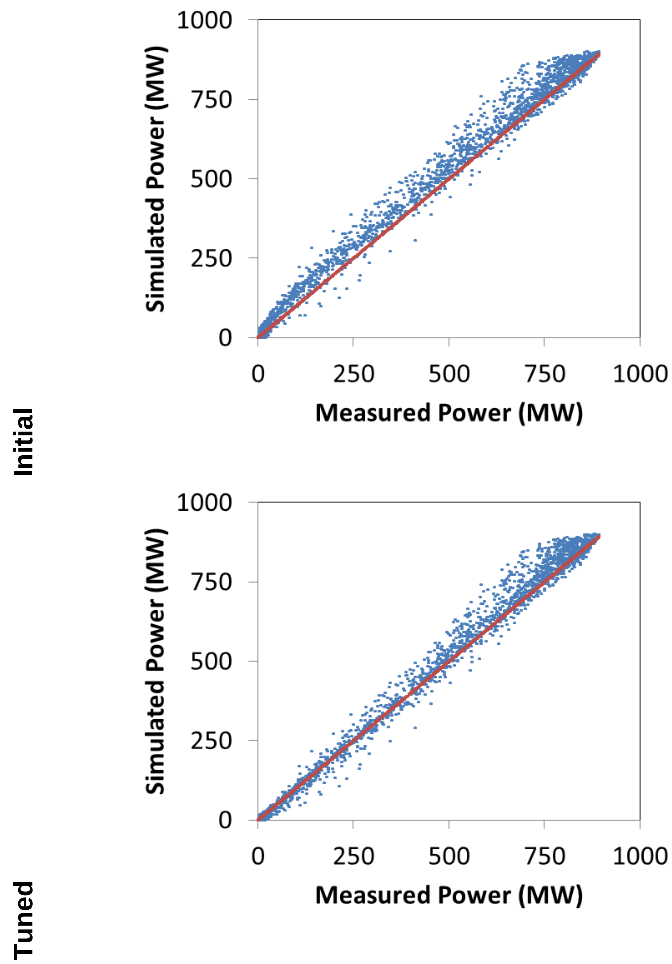

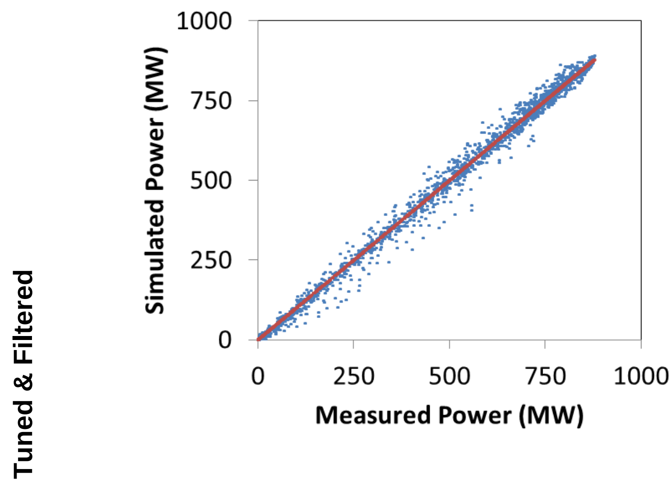

Figure 23: Power-Based Simulation Tuning

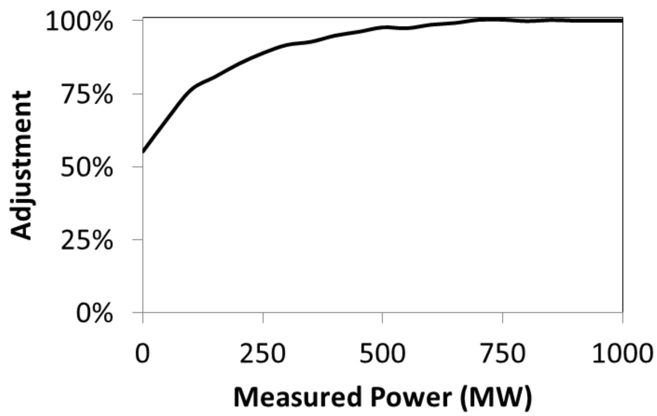

4.3.4 Relative Mean Absolute Error

The final step of the analysis is to calculate the rMAE. The time series data were evaluated over the approximately six-week time period for the 15-minute time interval data. Figure 24 presents results for three cases: Initial, Tuned, and Tuned & Filtered. These cases correspond to the results presented in Figure 22. Results show that the Initial, Tuned and, Tuned & Filtered cases have 7.2, 5.2, and 3.1 percent rMAE.

Several observations can be made based on these results. First, overall, FleetView PV power modeling is pretty accurate. There is, however, room for improvement. In particular, improving the inverter power curve model for individual PV systems will substantially improve simulation results (i.e., the improvement identified by applying the tuning).

Second, there is a substantially negative effect due to poorly performing plants even after the PV fleet model has been tuned. Accurately representing plant status reduces error by more than 40 percent.

Third, three percent rMAE can be achieved for 15-minute time interval data using a well-tuned model that accounts for poor PV plant performance. This requires that: (1) accurate location-specific solar resource data is supplied; (2) correct PV specifications are used; (3) the inverter power curve is properly represented (i.e., the simulation is tuned); and (4) actual PV plant status is incorporated into the simulation.

Figure 24: Total rMAE

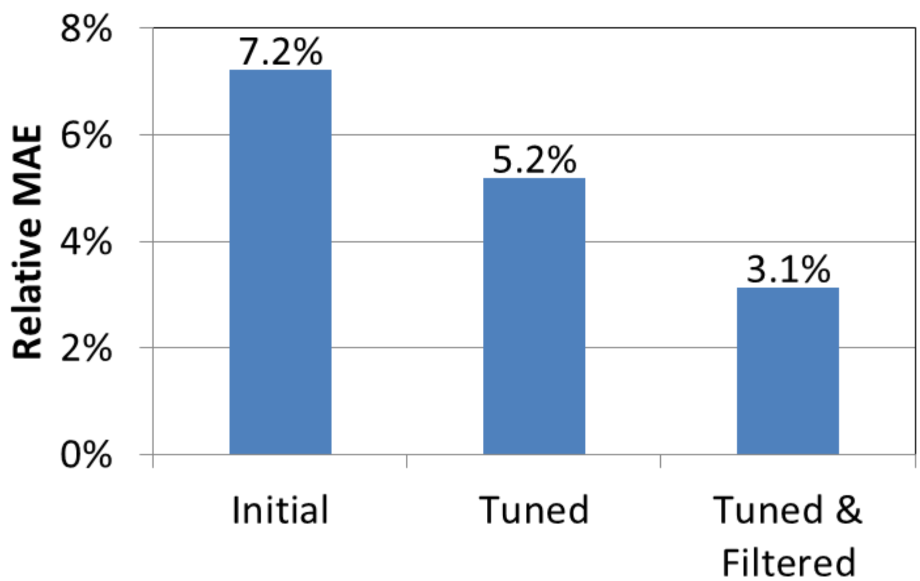

It is useful investigate the error on a daily basis in addition to an analysis over the entire time period. Figure 25 and Figure 26 presents the daily rMAE for the 15-minute time interval before and after tuning the model. The blue and red colors correspond to simulation error and PV plant performance error respectively. PV plant performance error is estimated by subtracting simulation error with and without filtering. The figure shows that rMAE varies from day to day. While absolute error increases on some of days, rMAE tends to be higher on low energy days. This is because the rMAE calculation is defined as absolute error divided by measured energy.

Figure 25: Daily Relative MAE Using 15-Minute Time Interval before Tuning

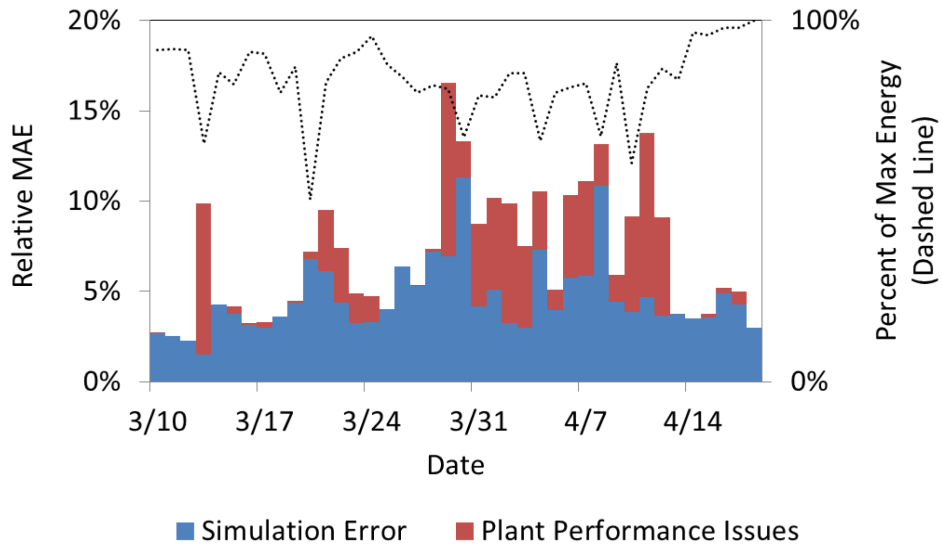

Figure 26: Daily Relative MAE Using 15-Minute Time Interval after Tuning

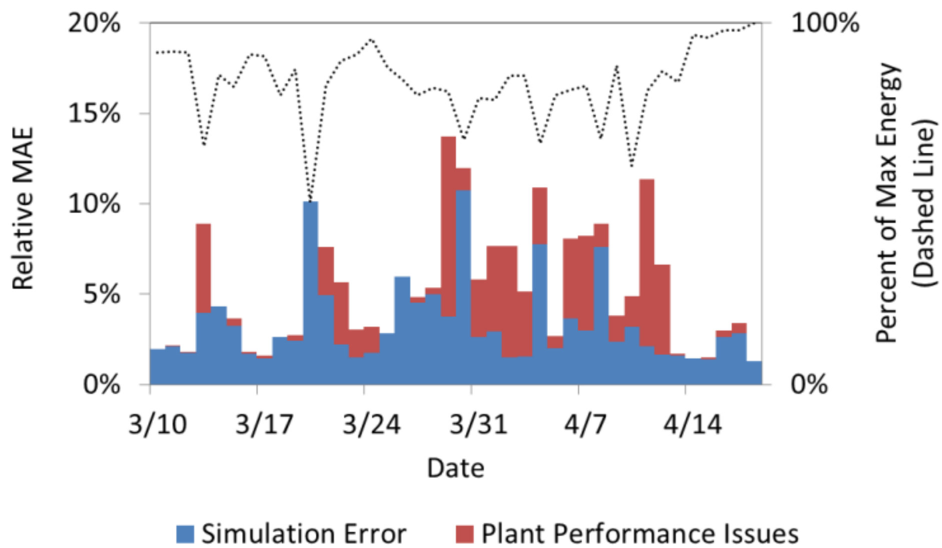

4.3.5 Sample Days After Tuning and Filtering

It is useful to compare simulated and measured data for a range of days after tuning and filtering. Figure 27, Figure 28, and Figure 29 present measured and simulated PV fleet production. Figure 27 corresponds to a clear day. Figure 28 corresponds to a day with PV performance issues. Figure 29 corresponds to a day with variable weather and PV performance issues.

Several observations can be made. First, tuning the simulation model increases accuracy for all days. Second, modeling on a clear day is very good with a rMAE of less than 2 percent. Third, filtering for PV plant performance issues can be very important; rMAE was reduced from 20 percent to 4 percent on one particular day. Fourth, simulated data tracks measured data fairly well even for the worst performing day.

Figure 27: PV Fleet Production on Clear Day

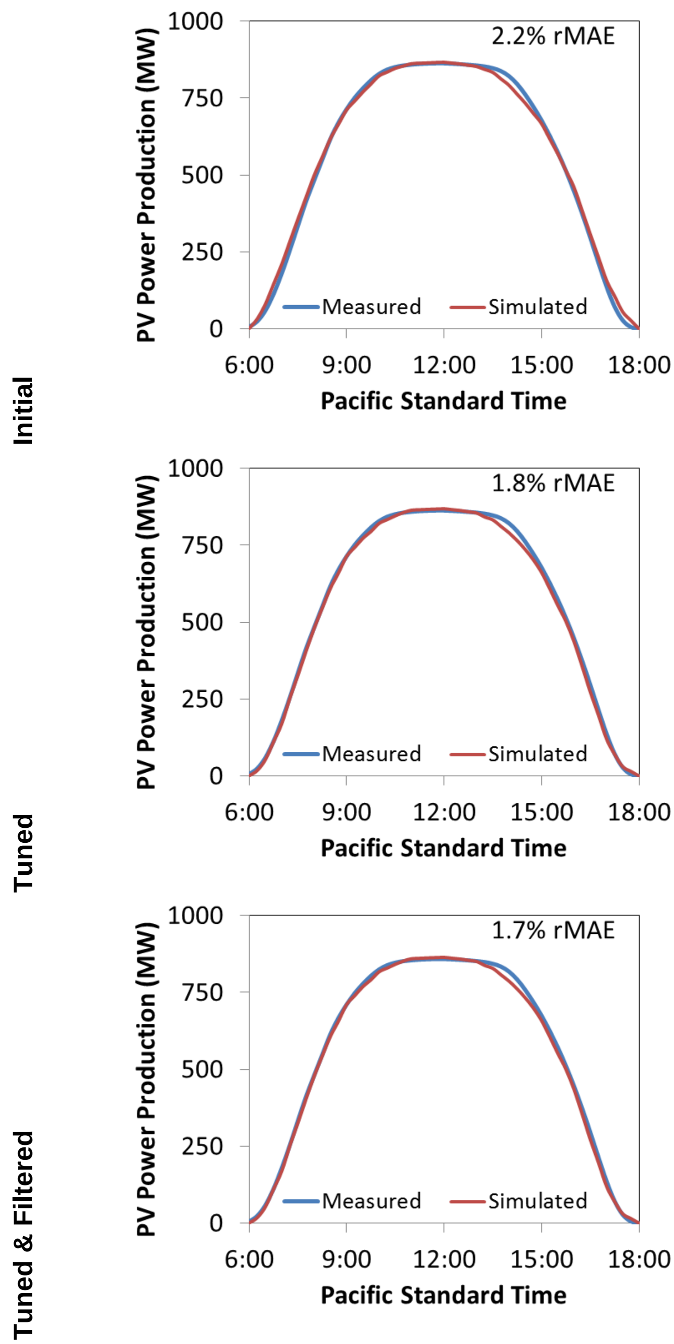

(March 12, 2013)

Figure 28: PV Fleet Production on Day with Production Issues

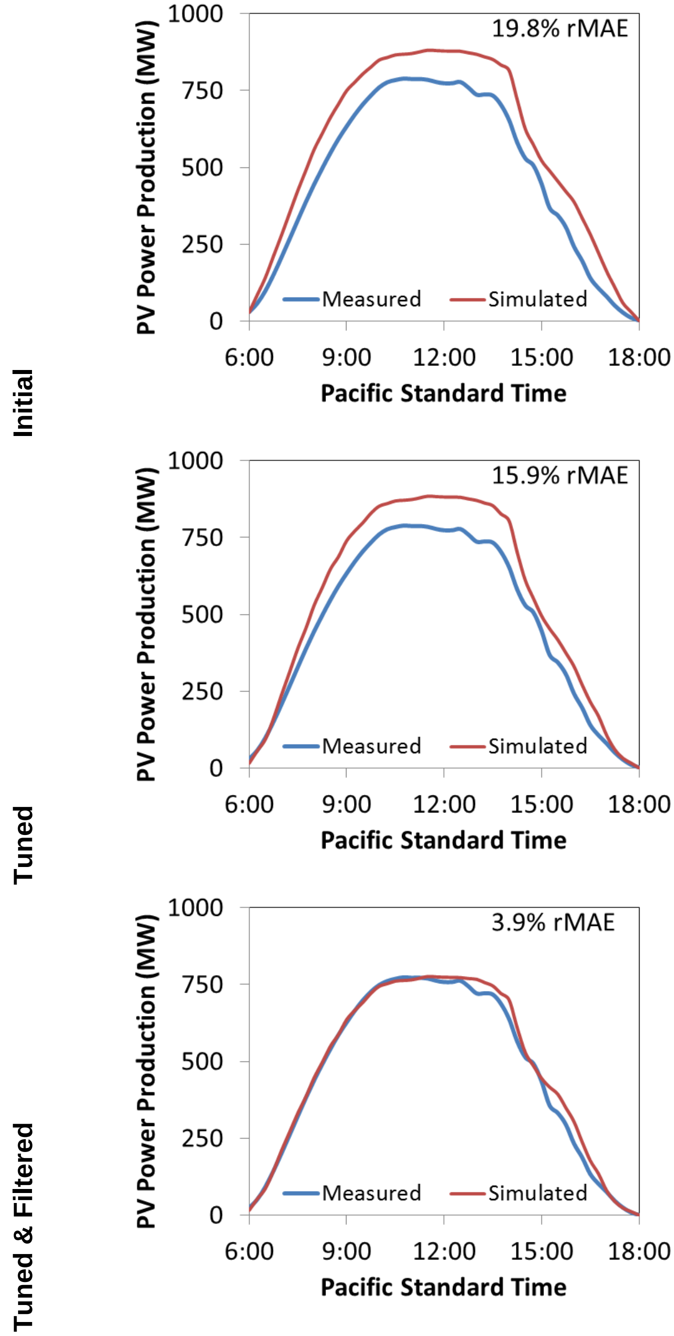

(March 29, 2013)

Figure 29: PV Fleet Production on Variable Weather Day with Production Issues

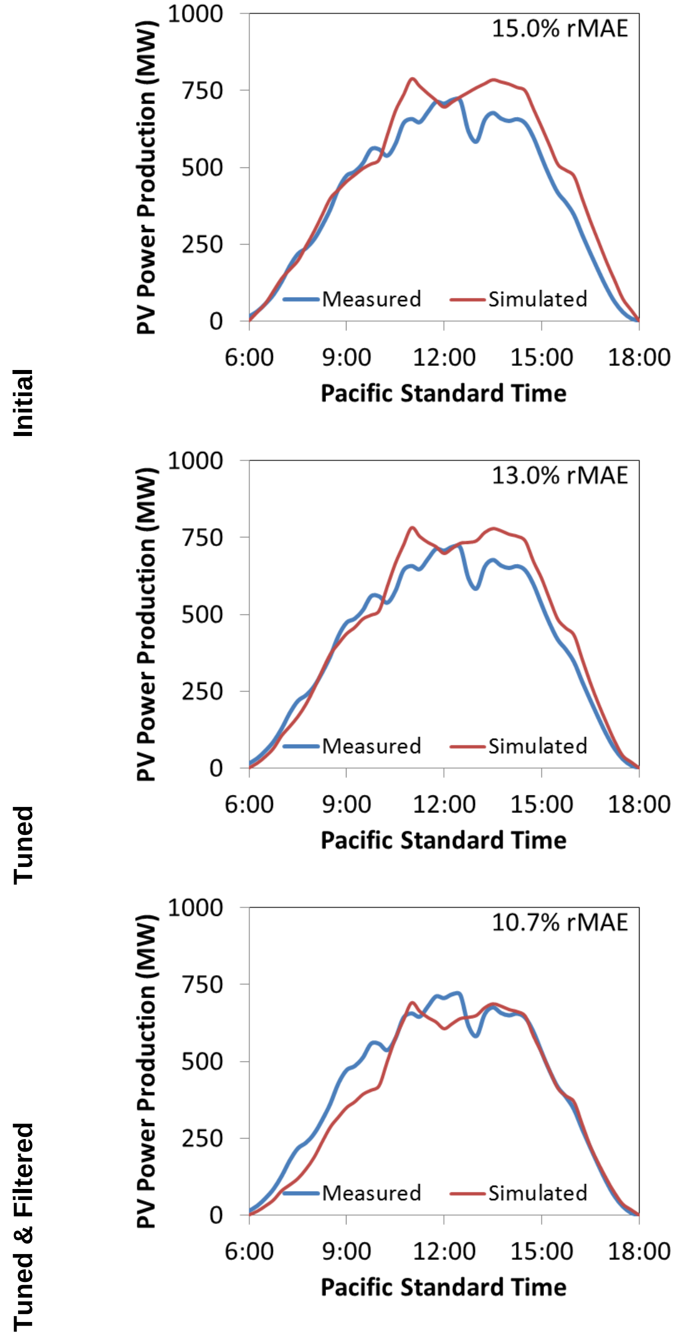

(March 29, 2013)

Chapter 5: Conclusions and Future Research

5.1 Conclusions

CPR has developed a unique method to predict PV fleet power production. The method uses inputs of satellite-derived solar resource data and the design attributes and locations of PV systems. It combines these inputs with advanced algorithms to track cloud patterns to predict output.

The objective of this project was to validate simulated PV fleet power production using measured PV fleet power production. This required:

- Obtaining PV system specifications for all PV systems in California.
- Obtaining solar resource data for the location of each PV system.
- Obtaining measured PV power production data for a subset of the fleet of systems.
- Screening the measured data for performance issues.
- Simulating PV fleet output using SolarAnywhere FleetView.
- Comparing measured and simulated results.

Results suggest that 3 percent Relative Mean Absolute Error (rMAE) can be achieved for 15-minute time interval data given that:

- Accurate location-specific solar resource data is supplied.
- Correct PV specifications are used.
- The PV simulation model is properly tuned.
- PV plant operating status is reflected in the simulation to account for poor performance.

Total error can be caused by solar resource inaccuracies, PV simulation model inaccuracies, and PV plant performance issues. Results also suggest that total error was over 7 percent if the model was not tuned and PV plant operating status was not reflected in the simulation.

This research also has the following benefits to CAISO:

- Prediction of behind-the-meter PV fleet performance for 1st time
- Fleet forecasts categorized by CAISO's five regions for both behind-the-meter and metered PV
- Gained confidence in CPR's PV fleet simulation accuracy
- Gained understanding into performance of metered PV plants
- Positioned to begin evaluation of integration of PV fleet forecasts into load forecasts
- PV fleet prediction tools available to support for PV fleet forecasting
- PV fleet prediction tools available to produce data required for high PV penetration grid planning

5.2 Future Research

There are several areas of future research.

- Improve inverter power curve modeling to reduce the need for tuning.
- Implement SolarAnywhere Enhanced Resolution data in Arizona to increase solar resource data resolution for all plants (i.e., Arizona plants, which represent almost half of the measured fleet capacity, currently use Standard Resolution data).
- Expand the analysis to incorporate solar resource forecast error.
- Incorporate PV plant performance status into the simulation to reduce total error.
- Continue validation efforts, especially during worst case conditions, to provide guidance as to how to use the data and to identify areas for improvement.
- Expand the analysis to probabilistic forecasting.
- Continue efforts to integrate results in to the CAISO processes.

REFERENCES

[1]. Lorentz E., T. Scheidsteger, J. Hurka, D. Heinemann and C. Kurz, (2011): Regional PV power prediction for improved grid integration. Progress in Photovoltaics, 19, 7, 757-771.

[2]. Hoff, T. E., Perez, R. 2010. "Quantifying PV power Output Variability." Solar Energy 84 (2010) 1782–1793.

[3]. Hoff, T. E., Perez, R. 2012. "Modeling PV Fleet Output Variability." Solar Energy 86 (2012) 2177–2189.

[4]. Kuszamaul, S., Ellis, A., Stein, J., Johnson, L. 2010. "Lanai High-Density Irradiance Sensor Network for Characterizing Solar Resource Variability of MW-Scale PV System." 35th Photovoltaic Specialists Conference, Honolulu, HI. June 20-25, 2010.

[5]. Mills, A., Wiser, R. 2010. Implications of Wide-Area Geographic Diversity for Short-Term Variability of Solar Power. Lawrence Berkeley National Laboratory Technical Report LBNL-3884E.

[6]. Mills, A., Ahlstrom, M., Brower, M., Ellis, A., George, R., Hoff, T., Kroposki, B., Lenox, C., Miller, N., Stein, J., Wan, Y., 2009. Understanding variability and uncertainty of photovoltaics for integration with the electric power system. Lawrence Berkeley National Laboratory Technical Report LBNL-2855E.

[7]. Navigant, Sandia National Laboratories, and Pacific Northwest National Laboratory. 2011. Large-Scale PV Integration Study. Report.

[8]. Norris, B. L., Hoff, T. E., 2011. "Determining Storage Reserves for Regulating Solar Variability." Electrical Energy Storage Applications and Technologies Biennial International Conference 2011.

[9]. Perez, R., Hoff, T.E. 2011. "Solar Resource Variability: Myth and Fact." Solar Today, August/September 2011.

[10]. Perez, R., Kivalov, S., Schlemmer, J., Hemker Jr., C. , Hoff, T. E. 2011. Parameterization of site-specific short-term irradiance variability, Solar Energy 85 (2011) 1343-1353.

[11]. Perez, R., Kivalov, S., Schlemmer, J., Hemker Jr., C. , Hoff, T. E. 2010b. "Short-term irradiance variability correlation as a function of distance." Accepted to Solar Energy (Feb. 2011).

[12]. Woyte, A., Belmans, R., Nijs, J. 2007. "Fluctuations in instantaneous clearness index: Analysis and statistics." Solar Energy 81 (2), 195-206.

[13]. Hoff, T. E. (2011). U.S. Patent Applications: Computer-Implemented System and Method for Determining Point-to-Point Correlation of Sky Clearness for Photovoltaic Power Generation Fleet Output Estimation (Application Number 13/190,435), Computer-Implemented System and Method for Estimating Power Data for a Photovoltaic Power Generation Fleet (Application Number 13/190,442), Computer-Implemented System and Method for Efficiently Performing

Area-to-Point Conversion of Satellite Imagery for Photovoltaic Power Generation Fleet Output Estimation(Application Number 13/190,449).

[14]. Solar Anywhere, 2012. Web-Based Service that Provides Hourly, Satellite-Derived Solar Irradiance Data Forecasted 7 days ahead and Archival Data back to January 1, 1998. www.SolarAnywhere.com.

[15]. Perez, R., T. Hoff and S. Kivalov, (2011): Spatial & temporal characteristics of solar radiation variability. Proc. of International Solar Energy (ISES) World Congress, Kassel, Germany

[16]. Jamaly, S., Bosch, J., Kleissl, J. 2012. "Aggregate Ramp Rates of Distributed Photovoltaic Systems in San Diego County." Submitted to IEEE Transactions on Sustainable Energy.

[17]. Willmott CJ, Ackleson SG, Davi RE, Feddema JJ, Klink KM, Legates DR, O'Donnell J, Rowe CM (1985) "Statistics for the evaluation and comparison of models." J. Geophys. Res. 90C: 8995-9005

[18]. IEA Solar Heating and Cooling Programme, Task 36, Subtask A, (2011): Standard Qualification for Solar Resource Products.

[19]. Hoff, T.E., Perez, R., Kleissl, J., Renne, D. Stein, J. 2012. "Reporting of Relative Irradiance Prediction Dispersion Error." American Solar Energy Society Annual Conference. May 2012. Denver, Co.

[20]. California Independent System Operator monitoring program (2011).

[21]. Ross, S. (1988). A First Course in Probability. Macmillan Publishing Company.

[22]. MESOR, 2002-2010 – Management and Exploitation of Solar Resource Knowledge. European Commission's Community Research Sixth Framework Programme.

[23]. IEA Solar Heating and Cooling Programme, Task 36, Subtask A, (2011): Standard Qualification for Solar Resource Products.

[24]. Beyer G. G., J. Polo Martinez, M. Suri, J. L. Torres, E. Lorenz, S. Muller, C. Hoyer-Klick and P. Ineichen, (2009): Benchmarking of Radiation Products, Mesor Report D.1.1.3.

[25]. Espinar B., L. Ramirez, A. Drews, H. G. Beyer, L. Zarzalejo, J. Polo Martinez and L. Martin, (2009): Analysis of Different Comparison Parameters Applied to Solar Radiation from Satellite and German Radiometric Stations.

[26]. Perez, R., M. Beauharnois, K. Hemker Jr., S. Kivalov, E. Lorenz, S. Pelland, J. Schlemmer, and G. Van Knowe, (2011): Evaluation of Numerical Weather Prediction Solar Irradiance Forecasts in the US. Proc. Solar 2011, American Solar Energy Society's Annual Conference.

[27]. Tastu, J., P. Oinson, E. Kotwa, H. Madsen and H. Nielsen, (2010): Spatio-Temporal Analaysis and Modeling of Short-Term Wind Power Forecast Errors. Wind Energy, 14, 43-60.

[28]. Integrated Surface Irradiance Study (ISIS) Network, (1995-2011).

Appendix A: Reporting of Relative Irradiance Prediction Dispersion Error

Introduction

Statistical methods for calculating and quantifying error have long been established across a wide range of sciences and industries. Whether quantifying the accuracy of an electrical meter, the tolerance of a precision part, or the expected range of forecasted temperatures, the methods for determining error are generally accepted. It is somewhat surprising, then, that these same methods have proved confusing and sometimes misleading when applied to commonly used diurnal quantities in the solar energy field.

Error calculations related to solar irradiance and PV power production, for example, are complicated by observations taken during nighttime and other low solar conditions. These conditions are often of little interest to the solar researcher, but they do cover the majority of time over a multi-day test period. Since these observations are subject to very low absolute error, their inclusion and weighting have a large impact on overall relative error.

As part of recent European and International Energy Agency (IEA) tasks [22], [23], a group of experts have developed recommendations for reporting irradiance model accuracy [24], [25]. Root Mean Square Error (RMSE), Mean Bias Error (MBE) and Kolmogorov Smirnoff Integral (KSI) are the three key recommended validation metrics. These respectively provide a measure of model's dispersion (RMSE), overall bias (MBE), and ability to reproduce observed frequency distributions (KSI).

In many contexts, however, relative error is more commonly desired than absolute error. While the IEA tasks developed recommendations for absolute errors, they have not developed recommendations on how to calculate error in percentage terms, aside from using the informally (but not universally) accepted approach of dividing RMSE by the day-time mean of the considered irradiance. This is unfortunate because users in the utility industry desire to understand error in relative terms rather than absolute terms.

A simplified reporting approach for the %KSI metric was proposed in a recent article [26]. The present note focuses on the relative dispersion error metrics (RMSE and MAE) with the objective of setting a standard for reporting these metrics in the industry and research community to facilitate comparison between forecast models.

Forecast model error also depends on meteorological conditions, forecast horizon, and averaging interval. There is not an attempt to create a metric that makes forecasts comparable across these dependencies. Rather, the focus is on which metric should be chosen to compare two forecasts at the same site, same forecast horizon, and same averaging interval. This discussion only focuses on methods concerned with expressing the relative error between two time series with a single statistic.

It should be remembered that methods that calculate relative or absolute error for each value in the time series may be more useful in practice, since they can uncover patterns that are obscured when the error for time series prediction is lumped into a single statistic.

Absolute errors

Root Mean Square Error (RMSE)

The RMSE is defined to be the square root of the sum of the squares of the difference between modeled and reference irradiances using some time interval (e.g., hourly) over some time period (e.g., one year) divided by the number of observations.

$$RMSE = \sqrt{\frac{\sum_{t=1}^{N}\left(I_t^{test} - I_t^{ref}\right)^2}{N}} \tag{3}$$

where I_t^{test} is the test irradiance at time t, I_t^{ref} is the reference irradiance at time t, and N is the number of observations.

One ambiguity with the RMSE calculation (as well as all other error calculations that involve any sort of averaging) is that a decision is required as to whether or not to include all values. The prevalent practice in the solar resource community has been to only include daytime values, sometimes filtered by solar zenith angle less than 80˚ to avoid shading and/or sensor cosine response issues under low sun angles.

Mean Absolute Error (MAE)

The MAE is defined to be the sum of the differences between modeled and reference irradiances using some time interval over some time period divided by the number of observations.

$$MAE = \frac{\sum_{t=1}^{N}\left|I_t^{test} - I_t^{ref}\right|}{N} \tag{4}$$

Relative (Percent) Errors

Quantifying relative error requires that absolute error (i.e., RMSE or MAE) be divided by a normalizing number. To emphasize, the normalization is not carried out for each I_t^{test} and I_t^{ref} pair, but rather using a single number representative of typical irradiances during the entire time series. Three possible candidates to use in the denominator to calculate *Percent Error* are:

- Average irradiance (Avg.).
- Weighted average irradiance (Weighted Avg.).
- Maximum nominal irradiance (Capacity).

Average

Average irradiance equals the sum of the irradiance values divided by the number of observations.

$$Average = \frac{\sum_{t=1}^{N} I_t^{ref}}{N} \quad (5)$$

Weighted Average

Weighted Average irradiance may be used to assign more importance to high-level irradiance observations. It is defined to be the sum of the irradiance values weighted by a factor.

$$Weighted\ Average = \sum_{t=1}^{N} W_t I_t^{ref} \quad (6)$$

One meaningful way to weight the irradiance is by its magnitude. That is, let

$$W_t = \frac{I_t^{ref}}{\sum_{t=1}^{N} I_t^{ref}} \quad (7)$$

Substituting Equation (7) into Equation (6) results in a Weighted Average of

$$Weighted\ Average = \frac{\sum_{t=1}^{N} \left(I_t^{ref}\right)^2}{\sum_{t=1}^{N} I_t^{ref}} \quad (8)$$

Unlike for the simple average, the day-time weighted average equals the 24-hour weighted averages since the weight of night-time points is zero.

Capacity

A third option is the peak irradiance or Capacity (C). For global horizontal irradiance, for example, the Capacity would be 1,000 W/m^2.

The wind industry has adopted this approach of normalizing to installed generating capacity for the reporting of output prediction errors [27].

Percent Error Calculation Methods

With two measures of dispersion (RMSE and MAE) and three normalizing means, there are six possible methods to calculate *Percent Error*. These methods are summarized in Table 8.

Table 9 presents the mathematical definitions used to calculate *Percent Error* by combining Equations (3) through (8) (see appendix for the detailed derivations).

Table 8: Possible *Percent Error* Calculation Methods

	RMSE	MAE
Average	RMSE/Avg.	MAE/Avg.
Weighted Average	RMSE/Weighted Avg.	MAE/Weighted Avg.
Capacity	RMSE/Capacity	MAE/Capacity

Table 9: Mathematical Definitions of *Percent Error* Methods

Percent Error Method	Definition	
RMSE/Avg.	$\sqrt{N}\left(\frac{1}{\sum_{t=1}^{N} I_t^{ref}}\right)$	$\sqrt{\sum_{t=1}^{N}\left(I_t^{test} - I_t^{ref}\right)^2}$
RMSE/Weighted Avg.	$\left[\frac{1}{\sqrt{N}}\right]\left[\frac{\sum_{t=1}^{N} I_t^{ref}}{\sum_{t=1}^{N}\left(I_t^{ref}\right)^2}\right]$	$\sqrt{\sum_{t=1}^{N}\left(I_t^{test} - I_t^{ref}\right)^2}$
RMSE/Capacity	$\left(\frac{1}{\sqrt{N}}\right)\left(\frac{1}{C}\right)$	$\sqrt{\sum_{t=1}^{N}\left(I_t^{test} - I_t^{ref}\right)^2}$
MAE/Avg.	$\left(\frac{1}{\sum_{t=1}^{N} I_t^{ref}}\right)$	$\sum_{t=1}^{N}\left\|I_t^{test} - I_t^{ref}\right\|$
MAE/Weighted Avg.	$\left[\frac{1}{N}\right]\left[\frac{\sum_{t=1}^{N} I_t^{ref}}{\sum_{t=1}^{N}\left(I_t^{ref}\right)^2}\right]$	$\sum_{t=1}^{N}\left\|I_t^{test} - I_t^{ref}\right\|$
MAE/Capacity	$\left(\frac{1}{N}\right)\left(\frac{1}{C}\right)$	$\sum_{t=1}^{N}\left\|I_t^{test} - I_t^{ref}\right\|$

24 Hours vs. Daytime

The effect of including 24 hours in the analysis vs. only including daytime values can be analyzed using the equations presented in

Table 9. *Total Error* (i.e., $\sqrt{\sum_{t=1}^{N}\left(I_t^{test}-I_t^{ref}\right)^2}$ or $\sum_{t=1}^{N}\left|I_t^{test}-I_t^{ref}\right|$) remains unchanged by including night-time values. However, *Absolute Error* (RMSE or MAE) is affected by the distinction since the results are obtained by dividing *Total Error* by the number of considered points. *Percent Error* is further affected by the daytime vs. 24-hour distinction since the normalizing means are different.

Table 10 summarizes the impact of the distinction on the selected error reporting metrics. It shows that *Percent Error* calculated using RMSE/Avg. method increases from 24 hour to daytime, the MAE/Avg. is unchanged, and *Percent Error* calculated using the other four methods decreases.

In all of the changed scenarios, the change is a function of the fraction of daytime hours. For example, if there are 4,380 daytime hours in a 12-month test period, the fraction Daytime Hours is 0.5. If night time hours are considered, *Percent Error* calculated using RMSE/Avg. will increase by 41 percent ($\sqrt{\frac{1}{0.5}}$), *Percent Error* calculated using RMSE/Weighted Avg. will decrease by 29 percent ($\sqrt{0.5}$), and *Percent Error* calculated using MAE/Weighted Avg. or MAE/Capacity will decrease by 50 percent. The only method independent of nighttime hours is the MAE/Avg. method.

Table 10: Ratio of *Percent Error* Using All Hours to *Percent Error* Using Daytime Hours

Percent Error Method	Ratio of Daytime to 24h Percent Error			
	$\sqrt{\frac{N^{All\ Hours}}{N^{Daytime\ Hours}}}$	100% (No change)	$\sqrt{\frac{N^{Daytime\ Hours}}{N^{All\ Hours}}}$	$\frac{N^{Daytime\ Hours}}{N^{All\ Hours}}$
RMSE/Avg.	✓			
RMSE/Weighted Avg.			✓	
RMSE/Capacity			✓	
MAE/Avg.		✓		
MAE/Weighted Avg.				✓
MAE/ Capacity				✓

Application Example

An effective way to compare and contrast the six possible methods is to quantify results using an actual irradiance data set. Hourly satellite-derived global horizontal insolation (GHI) data was obtained for Hanford, CA, from January 1, 2010 to December 31, 2010. The reference data are from a high-quality ISIS ground site [28]. The modeled data are from a satellite-based irradiance service [14].

Figure 30 plots one year's worth of hourly modeled data vs. measured data. A perfect match would occur if all blue dots were on the red line. As can be seen from the figure, the selected modeled data are a good visual match to the reference data.

Figure 30: Irradiance Data for Hanford, CA, 2010

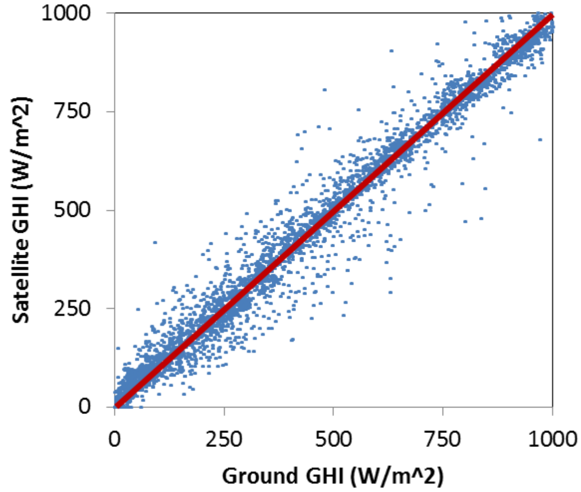

Figure 31 presents *Percent Error* for the six methods using the two scenarios of All Hours (24 hours per day) and Daytime Hours only. The "All Hours" scenarios are represented by the black bars. The "Daytime Hours" are represented by the white bars. Several observations can be made based on the figure:

- *Percent Error* ranges by a factor of more than 10 depending upon which method and scenario is selected
  - RMSE/Avg. method using nighttime values results in a 17.0 *Percent Error.*
  - MAE/Capacity method using nighttime values results in 1.5 *Percent Error*.
- The exclusion/inclusion of nighttime values changes results for five of the six definitions; *Percent Error* is lower for one case and higher for four cases.
- Only the MAE/Avg. *Percent Error* definition is independent of the inclusion of nighttime data.

Figure 31: Comparison of Error Results for Six Methods Using "All Hours" and "Daytime Hours" for Hanford, CA, 2010

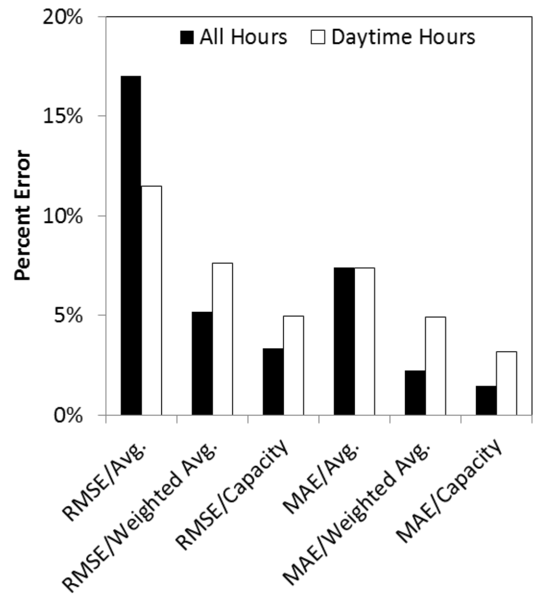

Threshold Dependence

The *Irradiance Threshold* is the value below which data are excluded. Use of a threshold is relevant because while the current practice is to exclude night-time values, the industry lacks a precise definition of what is night-time. Is night-time when irradiance is 0 W/m^2, 0.1 W/m^2, 1 W/m^2?

The 24-hour and daytime scenarios are specific threshold points, occurring respectively when irradiance is larger than, or equal to a zero *Irradiance Threshold* for the former and above the zero *Irradiance Threshold* for the latter.

Figure 32 presents the percent of solar energy that occurs below a given *Irradiance Threshold*. It is interesting to note that much of the collectable energy resides above significant threshold levels. For example, the dashed line shows that GHI observations less than an *Irradiance Threshold* of 250 W/m^2 correspond to only 8 percent of the annual GHI at Hanford, CA in 2010.

Figure 32: Energy Distribution of Irradiance Data for Hanford, CA, 2010

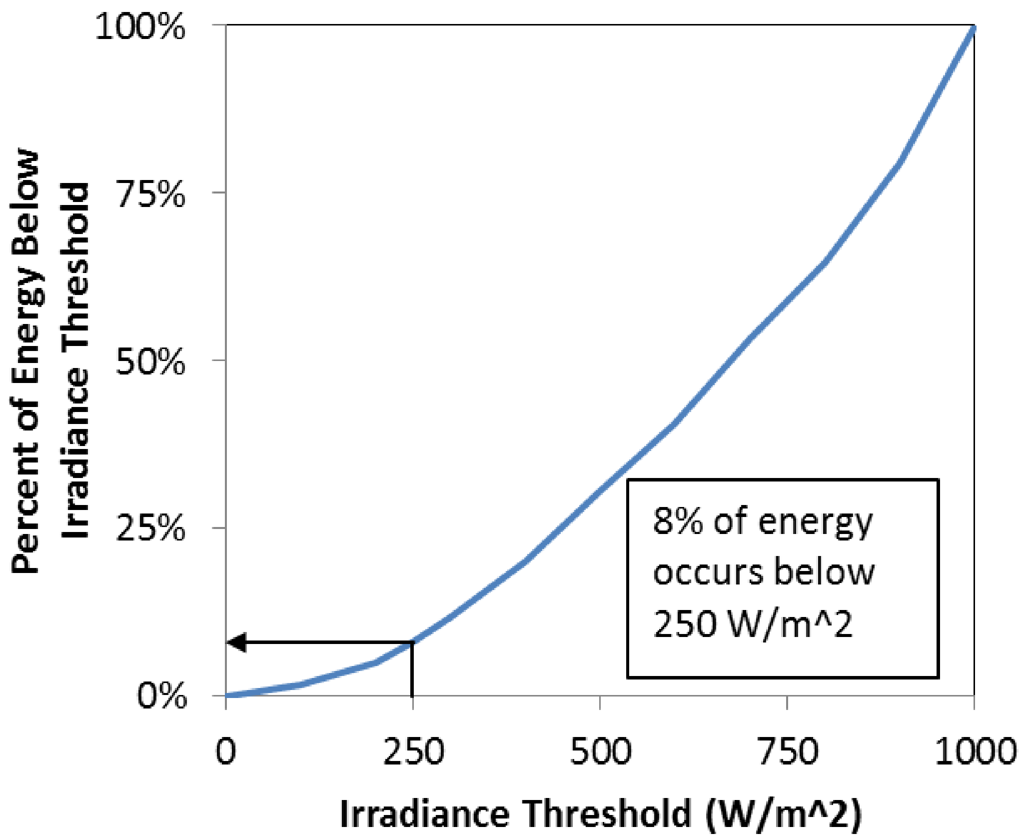

Figure 33 presents *Percent Error* as a function of *Irradiance Threshold* for all six methods. Several observations can be made based on the figure.

- All *Percent Error* definitions based on *RMSE* converge to the same result as the *Irradiance Threshold* increases.
- All *Percent Error* definitions based on *MAE* converge to the same result as the *Irradiance Threshold* increases.
- *RMSE/Weighted Avg.* results are similar to *MAE/Avg.* when "Daytime Hours" are included.

Figure 33: Comparison of Error Results for Hanford, CA, 2010

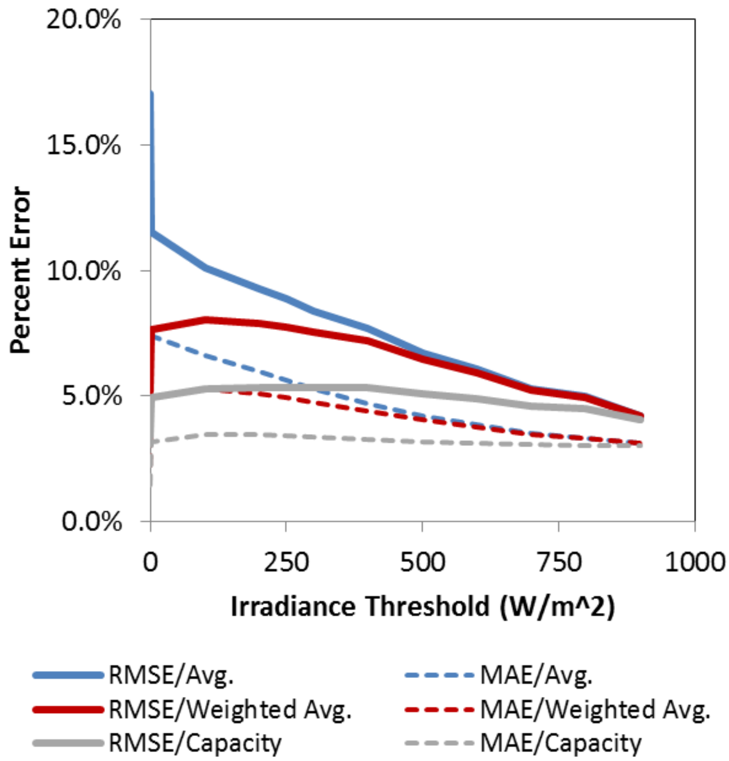

RMSE vs. MAE

Aside from the *Percent Error* reporting issue, it is worthwhile to explore the question whether the RMSE or the MAE is the most appropriate method to report dispersion error.

The main difference between the two is that the RMSE is driven by the square of the differences unlike the MAE. As a result, outliers are considerably more influential on the reported accuracy when using the RMSE metric. In the above example the addition of four far outliers to the data set (representing 0.1 percent of the data samples) increases the RMSE by a factor of 1.12, but only increases the MAE by a factor of 1.04.

Discussion

Table 4 summarizes the comparative observations made above using a subjective grading for the attributes of each relative dispersion error reporting method. The attributes we considered include:

- Whether the method is commonly accepted,
- Whether it is simple to understand
- Whether it depends on the 24-hr vs. daytime only distinction
- Whether it depends on the data selection threshold
- Whether it is affected by outliers

A grade of 0 to 2 is assigned to each method to represent its strength (2) or its weakness (0) with respect to a given attribute.

Table 11: Subjective Evaluation of Relative Error Reporting Method.

	Commonly accepted	Simple to understand	Depends on night time Values	Depends on selected threshold	Affected by outliers	Total
RMSE/Avg.	2	2	0	0	0	4
RMSE/Weighted Avg.	0	1	1	1	0	3
RMSE/Capacity	2	2	1	1	0	6
MAE/Avg.	1	2	2	1	1	7
MAE/Weighted Avg.	0	1	0	1	1	3
MAE/ Capacity	0	2	0	2	1	5

The MAE/Avg. provides the best practical measure of relative dispersion error based on the selected evaluation criteria and the subjective evaluations. The MAE/Avg. is attractive in that it is independent of the number of observations and is simple to understand. The RMSE/Capacity method is also desirable because it is commonly accepted (the wind power industry has already adopted this method) and is simple to understand.

The value of agreeing on a simple to calculate method has the benefit that multiple predictions and forecasts can be quickly evaluated and compared. Given that irradiance and PV power predictions and forecasts will be applied to a variety of applications (resource assessment, electrical grid operations and planning, etc.), it is not expected that the single statistic proposed here will necessarily be a complete measure of forecast quality. The authors, however feel that it is a good start towards promoting a standard metric in the industry.

Appendix B:
Percent Error Calculations

This appendix derives the Percent Error calculations based on the definitions of RMSE, MAE, Avg., Weighted Avg., and Capacity.

RMSE/Avg.

$$RMSE/Avg. = \frac{\sqrt{\frac{\sum_{t=1}^{N}\left(I_t^{test} - I_t^{ref}\right)^2}{N}}}{\frac{\sum_{t=1}^{N} I_t^{ref}}{N}} = \frac{\sqrt{N}}{\sum_{t=1}^{N} I_t^{ref}} \sqrt{\sum_{t=1}^{N}\left(I_t^{test} - I_t^{ref}\right)^2} \tag{9}$$

RMSE/Weighted Avg.

$$RMSE/Weighted\ Avg. = \frac{\sqrt{\frac{\sum_{t=1}^{N}\left(I_t^{test} - I_t^{ref}\right)^2}{N}}}{\frac{\sum_{t=1}^{N}\left(I_t^{ref}\right)^2}{\sum_{t=1}^{N} I_t^{ref}}} = \left[\frac{\sum_{t=1}^{N} I_t^{ref}}{\sqrt{N}\sum_{t=1}^{N}\left(I_t^{ref}\right)^2}\right] \sqrt{\sum_{t=1}^{N}\left(I_t^{test} - I_t^{ref}\right)^2} \tag{10}$$

RMSE/Capacity

$$RMSE/Capacity = \frac{\sqrt{\frac{\sum_{t=1}^{N}\left(I_t^{test} - I_t^{ref}\right)^2}{N}}}{\mathrm{C}} = \left(\frac{1}{C\sqrt{N}}\right) \sqrt{\sum_{t=1}^{N}\left(I_t^{test} - I_t^{ref}\right)^2} \tag{11}$$

MAE/Avg.

$$MAE/Avg. = \frac{\frac{\sum_{t=1}^{N}\left|I_t^{test} - I_t^{ref}\right|}{N}}{\frac{\sum_{t=1}^{N} I_t^{ref}}{N}} = \left(\frac{1}{\sum_{t=1}^{N} I_t^{ref}}\right) \sum_{t=1}^{N}\left|I_t^{test} - I_t^{ref}\right| \tag{12}$$

MAE/Weighted Avg.

$$MAE/Weighted\ Avg. = \frac{\frac{\sum_{t=1}^{N}\left|I_t^{test} - I_t^{ref}\right|}{N}}{\frac{\sum_{t=1}^{N}\left(I_t^{ref}\right)^2}{\sum_{t=1}^{N} I_t^{ref}}} = \left[\frac{\sum_{t=1}^{N} I_t^{ref}}{N\sum_{t=1}^{N}\left(I_t^{ref}\right)^2}\right]\sum_{t=1}^{N}\left|I_t^{test} - I_t^{ref}\right| \tag{13}$$

MAE/Capacity

$$MAE/Capacity = \frac{\frac{\sum_{t=1}^{N}\left|I_t^{test} - I_t^{ref}\right|}{N}}{\mathrm{C}} = \left(\frac{1}{CN}\right)\sum_{t=1}^{N}\left|I_t^{test} - I_t^{ref}\right| \tag{14}$$

Appendix C:
Half-hour Irradiance Data for Six CAISO Locations

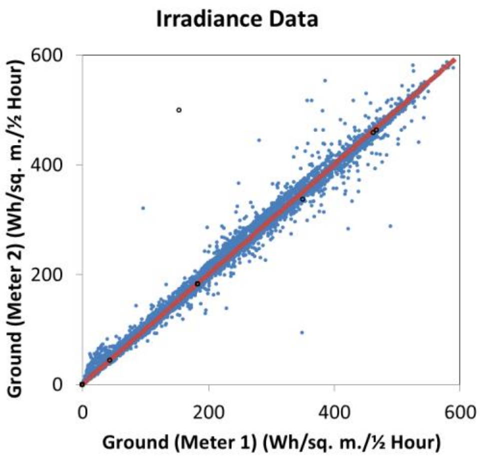

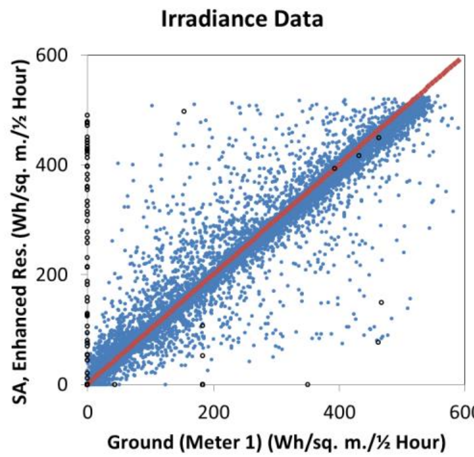

Site A

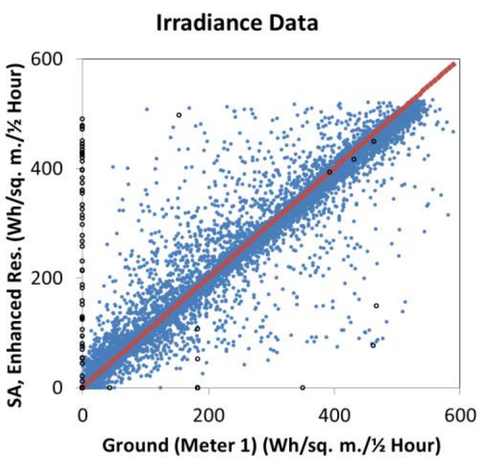

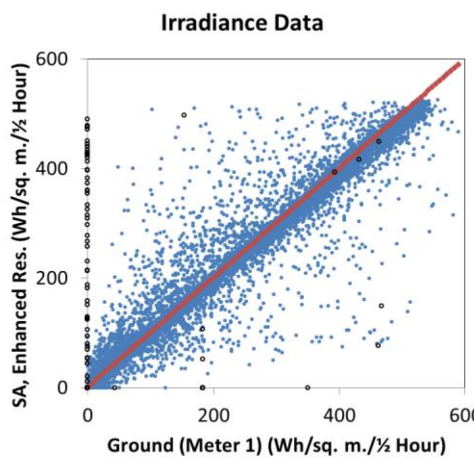

Site B

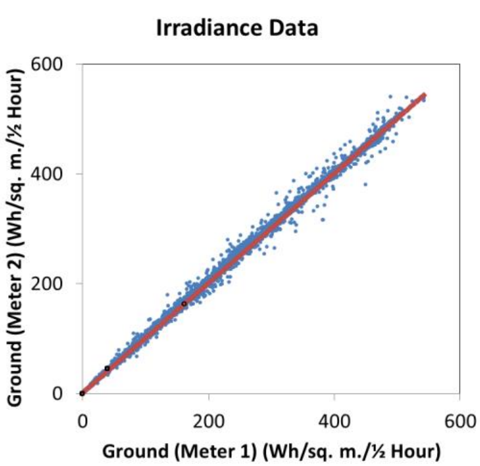

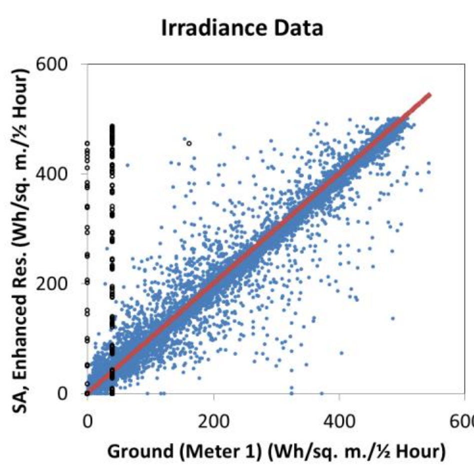

Site C

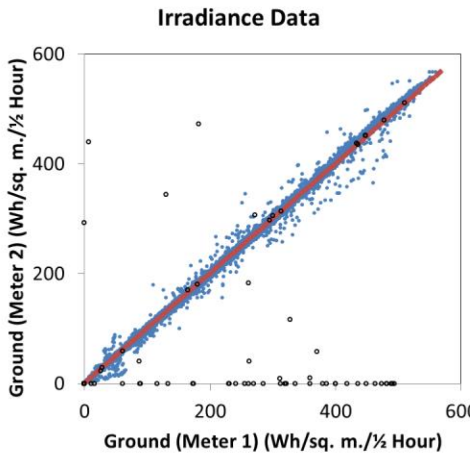

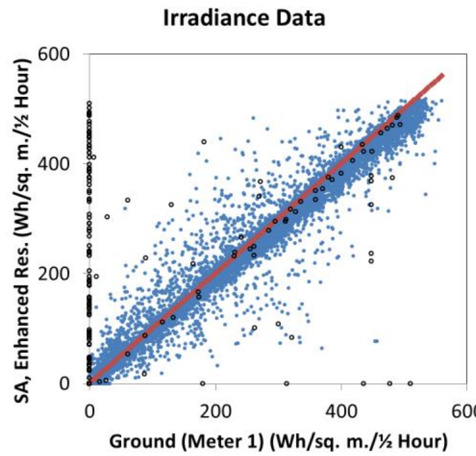

Site D

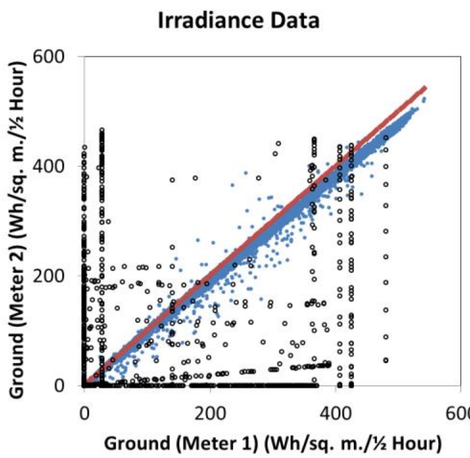

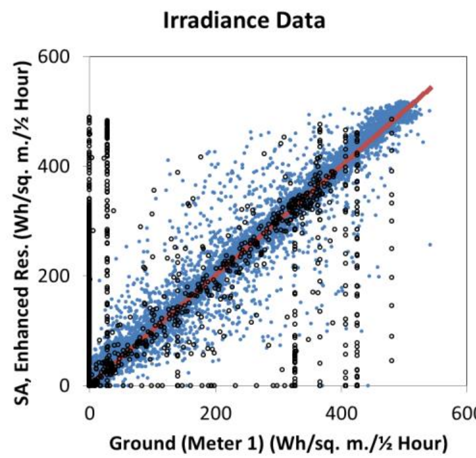

Site E

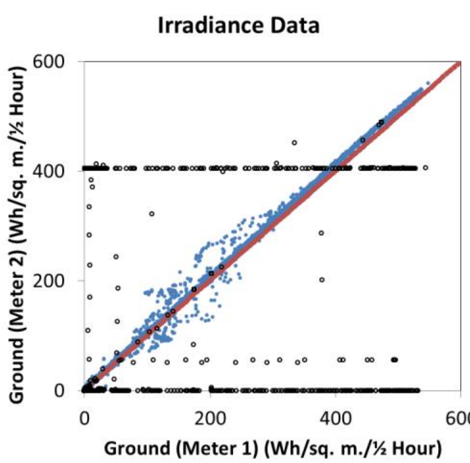

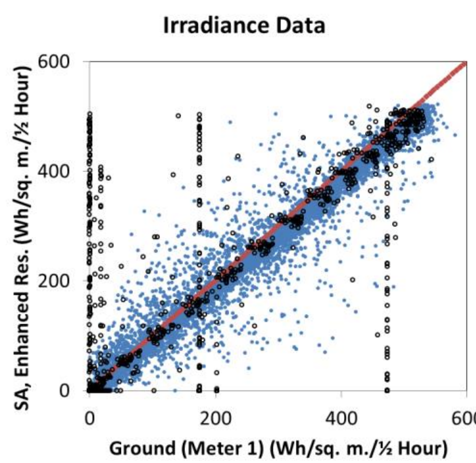

Site F